

# Distributional Variational AutoEncoder: To Infinite Quantiles and Beyond Gaussianity

SeungHwan An, Jong-June Jeon\*

Department of Statistics, University of Seoul, S. Korea  
{dkstmdghks79, jj.jeon}@uos.ac.kr

## Abstract

The Gaussianity assumption has been pointed out as the main limitation of the Variational AutoEncoder (VAE) in spite of its usefulness in computation. To improve the distributional capacity (i.e., expressive power of distributional family) of the VAE, we propose a new VAE learning method with a nonparametric distributional assumption on its generative model. By estimating an infinite number of conditional quantiles, our proposed VAE model directly estimates the conditional cumulative distribution function, and we call this approach distributional learning of the VAE. Furthermore, by adopting the continuous ranked probability score (CRPS) loss, our proposed learning method becomes computationally tractable. To evaluate how well the underlying distribution of the dataset is captured, we apply our model for synthetic data generation based on inverse transform sampling. Numerical results with real tabular datasets corroborate our arguments.

## 1 Introduction

Variational Autoencoder (VAE) Kingma & Welling (2013) and Generative Adversarial Networks (GAN) Goodfellow et al. (2014) are generative models that are used to estimate the underlying distribution of a given dataset. To avoid the curse of dimensionality, VAE and GAN commonly introduce a low-dimensional latent space on which a conditional generative model is defined. By minimizing an information divergence between the original data and its generated data, the generative models are learned to produce synthetic data similar to the original one. Accordingly, VAE and GAN have been applied in various applications, such as generating realistic images, texts, and synthetic tabular

data for privacy preservation purposes Karras et al. (2018); Wang et al. (2019); Xu et al. (2019); Zhao et al. (2021).

However, the difference in the strength of the assumption about the generative distribution brings significant contrasts in the VAE and GAN generation performances. In the GAN framework, the adversarial loss enables direct minimization of the Jensen-Shannon divergence between the ground-truth density function and the generative distribution under no distributional assumption. Roughly speaking, the GAN employs a nonparametric model as its conditional generative model defined on the latent space.

On the contrary, in the VAE framework, the Gaussianity assumption has been favored Lucas et al. (2019). It is because Gaussianity gives us three advantages: 1) the reconstruction loss can be interpreted as  $L_2$  loss which is one of the most popular losses in optimization theory, 2) generating a new sample is computationally straightforward, and 3) KL-divergence is computed in a simple closed form. However, these benefits have led us to pay the price for the distributional capacity of the generative model, in that the generative model of the VAE is constrained in the form of marginalization of the product of the two Gaussian distributions. Here, the distributional capacity means the expressive power of the distributional family. This restricted distributional capacity has been the critical limitation Burda et al. (2015); Kingma et al. (2016) and leads to a heavy parameterization of the decoder mean-vector to approximate complex underlying distributions.

To increase the distributional capacity in the VAE framework, Xu et al. (2019); Zhao et al. (2021) introduce the multi-modality in the distributional assumption of the decoder, which is known as the mode-specific normalization technique. Although the mixture-Gaussian decoder modeling of Xu et al. (2019)

\*Corresponding author.

allows handling more complex distributions of the observed dataset while preserving all of the advantages of Gaussianity, we numerically find that the mixture Gaussian is not enough to capture the underlying distribution.

Our main contribution is that, beyond Gaussianity, we propose a novel VAE learning method that directly estimates the conditional cumulative distribution function (CDF). It implies that we have a nonparametric distribution assumption on the VAE model. We call this approach distributional learning of the VAE, which is enabled by estimating an infinite number of conditional quantiles. By adopting the loss function of continuous ranked probability score (CRPS) used to estimate the CDF, the objective of the distribution learning is computationally tractable Gneiting & Raftery (2007); Matheson & Winkler (1976).

Therefore, in our proposed distributional learning framework, 1) the reconstruction loss can be interpreted as CRPS loss which is a well-known *proper scoring rule* Gneiting & Raftery (2007), 2) generating a new sample is still computationally straightforward due to inverse transform sampling, and 3) KL-divergence is still computed in a simple closed form. To show the effectiveness of our proposed model in capturing the underlying distribution of the dataset, we evaluate our model for synthetic data generation with real tabular datasets.

## 2 Related Work

**Various decoder modeling.** Decoder modeling has been primarily focused on increasing distributional capacity while maintaining the simple calculation of the KL-divergence. Takahashi et al. (2018); Akrami et al. (2020) assume their decoder distributions as Student- $t$  and asymmetric Laplace distributions, respectively. These assumptions mitigate the *zero-variance problem* that the model training becomes unstable if the estimated variance of the decoder shrinks to zero in Gaussian VAE. In the image domain, Gaussian assumption hinders the reconstruction of images and fails to capture the properties of human perception Larsen et al. (2015). Therefore, Larsen et al. (2015); Rosca et al. (2017); Munjal et al. (2019) replace the reconstruction loss with an adversarial loss, and the decoder is trained without a parametric distributional assumption. However, adopting adversarial loss induces unstable model training in general.

**Synthetic data generation.** The GAN framework is widely adopted in the synthetic data generation task since it enables handling columns of tabular datasets that are usually non-Gaussian Choi et al. (2017); Park

et al. (2018); Xu et al. (2019); Zhao et al. (2021). Especially, Xu et al. (2019); Zhao et al. (2021) assume their decoder as Gaussian mixture distribution and preprocess the continuous variables using the Variational Gaussian mixture model Blei et al. (2016), which is known as the mode-specific normalization technique. However, this preprocessing requires additional computational resources and hyperparameter tuning of the number of modes.

## 3 Proposal

Let  $\mathbf{x} \in \mathcal{X} \subset \mathbb{R}^p$  be an observation, where  $\mathbf{x}_1, \dots, \mathbf{x}_{p_1}$  are continuous random variables, and  $\mathbf{x}_{p_1+1}, \dots, \mathbf{x}_p$  are discrete random variables. Denote  $q(\mathbf{x})$  as the true underlying distribution defined over  $\mathbf{x} \in \mathcal{X}$ . Let  $\mathbf{z}$  be a latent variable, where  $\mathbf{z} \in \mathbb{R}^d$  and  $d < p$ . The prior and posterior distribution of  $\mathbf{z}$  is assumed as  $p(\mathbf{z}) = \mathcal{N}(\mathbf{z}|\mathbf{0}, I)$  and  $q(\mathbf{z}|\mathbf{x}; \phi) = \mathcal{N}(\mathbf{z}|\mu(\mathbf{x}; \phi), \text{diag}(\sigma^2(\mathbf{x}; \phi)))$ , respectively, where  $I$  is  $d \times d$  identity matrix,  $\phi$  is the neural network parameter, and  $\text{diag}(a), a \in \mathbb{R}^d$  denotes a diagonal matrix with diagonal elements  $a$ . Assume that there exists  $p(\mathbf{x}|\mathbf{z})$  such that  $q(\mathbf{x}) = \int p(\mathbf{z})p(\mathbf{x}|\mathbf{z})d\mathbf{z}$ .

In addition, let  $\alpha$  be a discrete random variable of which the possible values set is  $\{1/K, 2/K, \dots, (K-1)/K, 1\}$ .  $\alpha$  follows a discrete uniform distribution, and we denote  $\alpha_k := k/K$  for  $k = 1, \dots, K$ .

### 3.1 Model Assumptions

First, we assume that  $\mathbf{x}_1, \dots, \mathbf{x}_p$  are conditionally mutually independent given  $\mathbf{z}$ . The distribution of  $\mathbf{x}_j$  given  $\mathbf{z}$  and  $\alpha_k$  is assumed as the asymmetric Laplace distribution, for  $j = 1, 2, \dots, p_1$ . For  $l = p_1 + 1, p_1 + 2, \dots, p$ , the distribution of  $\mathbf{x}_l$  given  $\mathbf{z}$  is categorical distribution and the number of category of  $\mathbf{x}_l$  is denoted as  $T_l$ . Then, for  $k = 1, \dots, K$ , the decoder is written as

$$\begin{aligned} & p(\mathbf{x}|\mathbf{z}, \alpha_k; \theta, \beta) \\ &= \prod_{j=1}^{p_1} p(\mathbf{x}_j|\mathbf{z}, \alpha_k; \theta_j, \beta) \cdot \prod_{l=p_1+1}^p p(\mathbf{x}_l|\mathbf{z}; \theta_l, \beta) \\ &= \prod_{j=1}^{p_1} \frac{\alpha_k(1-\alpha_k)}{\beta} \exp\left(-\rho_{\alpha_k}\left(\frac{\mathbf{x}_j - D_j(\alpha_k|\mathbf{z}, \theta_j)}{\beta}\right)\right) \\ & \quad \cdot \prod_{l=p_1+1}^p \prod_{t=1}^{T_l} \pi(\mathbf{z}; \theta_l)_t^{I(\mathbf{x}_l=t)}, \end{aligned} \tag{1}$$

where  $\theta = (\theta_1, \dots, \theta_p)$ ,  $\beta$  is the non-trainable hyperparameter,  $\rho_v(\mathbf{u}) = \mathbf{u}(v - I(\mathbf{u} < 0))$  is the check

function, and  $I(\cdot)$  is indicator function.  $D_j(\cdot|\cdot, \theta_j) : [0, 1] \times \mathbb{R}^d \mapsto \mathbb{R}$  is location parameter of conditional distribution of continuous  $\mathbf{x}_j$ . Note that all continuous variables share the same scale parameter  $\beta$ . For discrete variables,  $\pi(\cdot; \theta_l) : \mathbb{R}^d \mapsto [0, 1]^{T_l}$  and  $\sum_{t=1}^{T_l} \pi(\mathbf{z}; \theta_l)_t = 1$ , for all  $\mathbf{z} \in \mathbb{R}^d$ .

With proposal distributions, the negative ELBO is written as

$$\begin{aligned} & \sum_{j=1}^{p_1} \mathbb{E}_{q(\mathbf{z}|\mathbf{x}; \phi)} \left[ \frac{1}{2 \cdot K} \sum_{k=1}^K 2 \cdot \rho_{\alpha_k}(\mathbf{x}_j - D_j(\alpha_k|\mathbf{z}, \theta_j)) \right] \\ & - \beta p_1 \frac{1}{K} \sum_{k=1}^K \log \alpha_k (1 - \alpha_k) + \beta p_1 \log \beta \\ & - \beta \cdot \sum_{l=p_1+1}^p \mathbb{E}_{q(\mathbf{z}|\mathbf{x}; \phi)} \left[ \sum_{t=1}^{T_l} I(\mathbf{x}_l = t) \cdot \log \pi(\mathbf{z}; \theta_l)_t \right] \\ & + \beta \cdot \mathcal{KL}(q(\mathbf{z}|\mathbf{x}; \phi) \| p(\mathbf{z})) \end{aligned} \quad (2)$$

(see Appendix A.1 for detailed derivation). Note that the reconstruction loss of (2) can be seen as estimating  $K$  multiple conditional quantiles in Bayesian framework Yu & Moyeed (2001); Moon et al. (2021), where  $\alpha_k$  plays the role of quantile level.

### 3.2 Distributional Learning

For distributional learning of the VAE, we need to estimate conditional quantiles for an infinite number of quantile levels, i.e.,  $K \rightarrow \infty$ . The following Proposition 1 shows that the negative ELBO (2) converges to the continuous ranked probability score (CRPS) loss, which measures how accurately the proposed CDF approximates the true CDF of the dataset.

**Proposition 1** (Convergence to CRPS). *Suppose that  $\int_0^1 \mathbb{E}_{q(\mathbf{z}|\mathbf{x}; \phi)} \left| 2 \cdot \rho_{\alpha}(\mathbf{x}_j - D_j(\alpha|\mathbf{z}, \theta_j)) \right| d\alpha < \infty$ . Then, for  $j = 1, \dots, p_1$ ,*

$$\begin{aligned} & \lim_{K \rightarrow \infty} \mathbb{E}_{q(\mathbf{z}|\mathbf{x}; \phi)} \left[ \frac{1}{K} \sum_{k=1}^K 2 \cdot \rho_{\alpha_k}(\mathbf{x}_j - D_j(\alpha_k|\mathbf{z}, \theta_j)) \right] \\ & = \mathbb{E}_{q(\mathbf{z}|\mathbf{x}; \phi)} \left[ \int_0^1 2 \cdot \rho_{\alpha}(\mathbf{x}_j - D_j(\alpha|\mathbf{z}, \theta_j)) d\alpha \right] \\ & = \mathbb{E}_{q(\mathbf{z}|\mathbf{x}; \phi)} [\text{CRPS}(D_j(\cdot|\mathbf{z}; \theta_j), \mathbf{x})], \end{aligned}$$

where  $\text{CRPS}(\cdot, \cdot)$  is the continuous ranked probability score (CRPS), and

$$\lim_{K \rightarrow \infty} \frac{1}{K} \sum_{k=1}^K \log \alpha_k (1 - \alpha_k) = \int_0^1 \log \alpha (1 - \alpha) d\alpha = -2.$$

Therefore, when  $K \rightarrow \infty$ , our final objective is minimizing

$$\begin{aligned} & \sum_{j=1}^{p_1} \mathbb{E}_{q(\mathbf{x})} \mathbb{E}_{q(\mathbf{z}|\mathbf{x}; \phi)} \left[ \frac{1}{2} \cdot \text{CRPS}(D_j(\cdot|\mathbf{z}; \theta_j), \mathbf{x}) \right] \\ & - \sum_{l=p_1+1}^p \mathbb{E}_{q(\mathbf{x})} \mathbb{E}_{q(\mathbf{z}|\mathbf{x}; \phi)} \left[ \sum_{t=1}^{T_l} I(\mathbf{x}_l = t) \cdot \log \pi(\mathbf{z}; \theta_l)_t \right] \\ & + \beta \cdot \mathbb{E}_{q(\mathbf{x})} [\mathcal{KL}(q(\mathbf{z}|\mathbf{x}; \phi) \| p(\mathbf{z}))] \end{aligned} \quad (3)$$

with respect to  $(\theta, \phi)$ , where constant terms are omitted. To balance the learning of two reconstruction losses in (3), we remove coefficient  $\beta$  of the second term, which is the reconstruction loss of discrete variables. We call our model DistVAE. In addition, see Appendix A.2 for the interpretation of distributional learning in terms of model misspecification error in MLE.

Higgins et al. (2016) shows that the KL-divergence coefficient  $\beta$  (the scale parameter of asymmetric Laplace distribution) controls the reconstruction precision. Since our reconstruction loss consists of CRPS loss, a larger  $\beta$  induces an inaccurate estimation of the true CDF, leading to a lower quality of synthetic data. Consequently, the privacy level will be lower if  $\beta$  is small. Therefore,  $\beta$  creates a trade-off between the synthetic data quality and the risk of privacy leakage, which means that the privacy level is controllable via  $\beta$  Park et al. (2018) (see Section 4).

#### 3.2.1 Proper Scoring Rule

In this section, we will show that the reconstruction loss of (3) is a *proper scoring rule* Gneiting & Raftery (2007) relative to the true conditional quantile function. Let  $F(\mathbf{x}|\mathbf{z})$  is CDF of  $p(\mathbf{x}|\mathbf{z})$  and denote  $F_j(\mathbf{x}_j|\mathbf{z})$  as the marginal conditional CDF of  $\mathbf{x}_j$ , for  $j = 1, \dots, p_1$ . Denote  $D_j^*(\alpha|\mathbf{z})$  as the true conditional  $\alpha$ -quantile with respect to  $F_j(\mathbf{x}_j|\mathbf{z})$  for  $\alpha \in (0, 1)$  and  $\mathbf{z} \in \mathbb{R}^d$ . It implies that  $F_j(D_j^*(\alpha|\mathbf{z})|\mathbf{z}) = \alpha$ . We define a risk functional of  $D_j \in \mathcal{D}_j$  by

$$\begin{aligned} \mathcal{S}_{\alpha}(D_j, D_j^*) &= \mathbb{E}_{q(\mathbf{x})} \mathbb{E}_{q(\mathbf{z}|\mathbf{x}; \phi)} \left[ \rho_{\alpha}(\mathbf{x}_j - D_j(\alpha|\mathbf{z})) \right] \\ \mathcal{S}(D_j, D_j^*) &= \mathbb{E}_{q(\mathbf{x})} \mathbb{E}_{q(\mathbf{z}|\mathbf{x}; \phi)} \left[ \int_0^1 \rho_{\alpha}(\mathbf{x}_j - D_j(\alpha|\mathbf{z})) d\alpha \right], \end{aligned}$$

where  $\alpha \in (0, 1)$ , and  $\mathcal{D}_j$  is a set of isotonic functions  $D_j$  such that  $D_j(\cdot|\cdot) : [0, 1] \times \mathbb{R}^d \mapsto \mathbb{R}$ . Note that  $\mathcal{S}(D_j, D_j^*)$  is equivalent to the reconstruction loss of (3).

**Assumption 1.** *The distributional family of  $q(\mathbf{z}|\mathbf{x}; \phi)$  is sufficiently large and we have  $q(\mathbf{z}|\mathbf{x}; \phi)$  such that*

$$q(\mathbf{x})q(\mathbf{z}|\mathbf{x}; \phi) = p(\mathbf{z})p(\mathbf{x}|\mathbf{z}).$$

**Proposition 2** (Proper scoring rule). *Suppose that  $\mathbb{E}_{q(\mathbf{x})}\mathbb{E}_{q(\mathbf{z}|\mathbf{x};\phi)}\left[\int_0^1|\rho_\alpha(\mathbf{x}_j - D_j(\alpha|\mathbf{z}))|d\alpha\right] < \infty$  for all  $D_j \in \mathcal{D}_j$ ,  $j = 1, \dots, p_1$ . Under Assumption 1, for all  $\alpha \in (0, 1)$ ,*

$$\mathbb{E}_{q(\mathbf{x})}\mathbb{E}_{q(\mathbf{z}|\mathbf{x};\phi)}\left[\rho_\alpha(\mathbf{x}_j - D_j^*(\alpha|\mathbf{z}))\right] = \min_{D_j \in \mathcal{D}_j} \mathcal{S}_\alpha(D_j, D_j^*),$$

and  $\mathcal{S}(D_j, D_j^*) \geq \mathcal{S}(D_j^*, D_j^*)$ .

Furthermore, based on the conditional CDF  $D_j^{-1}$ , the following Proposition 3 shows that the marginal CDF is equivalent to the marginalization of the conditional CDF with respect to the prior distribution.

**Proposition 3** (Marginal CDF). *For  $j = 1, 2, \dots, p_1$ , the marginal CDF  $F_j(x_j)$  of  $\mathbf{x}_j$  is written as*

$$F_j(x_j) = \int_{\mathbb{R}^d} D_j^{-1}(x_j|\mathbf{z})p(\mathbf{z})d\mathbf{z},$$

where  $x_j \in \mathbb{R}$ .

In practice, the marginal CDF  $F_j(x_j)$  is approximated by  $\frac{1}{B} \sum_{b=1}^B D_j^{-1}(x_j|z_b)$ , where  $z_b \sim p(\mathbf{z})$ ,  $b = 1, \dots, B$ .

### 3.2.2 Closed Form Loss

To compute the CRPS loss in the closed form for computational efficiency Gasthaus et al. (2019), we parameterize the function  $D_j$  by a linear isotonic regression spline as follows

$$D_j(\alpha|\mathbf{z}; \theta_j) = \gamma^{(j)}(\mathbf{z}) + \sum_{m=0}^M b_m^{(j)}(\mathbf{z})(\alpha - d_m)_+ \\ \text{subject to } \sum_{m=0}^k b_m^{(j)}(\mathbf{z}) \geq 0, k = 1, \dots, M \quad (4)$$

where  $\alpha \in [0, 1]$ ,  $\gamma^{(j)}(\mathbf{z}) \in \mathbb{R}$ ,  $b^{(j)}(\mathbf{z}) = (b_0^{(j)}(\mathbf{z}), \dots, b_M^{(j)}(\mathbf{z})) \in \mathbb{R}^{M+1}$ ,  $d = (d_0, \dots, d_M) \in [0, 1]^{M+1}$ ,  $0 = d_0 < \dots < d_M = 1$ , and  $(\mathbf{u})_+ := \max(0, \mathbf{u})$ .  $\theta_j$  is a neural network parameterized mapping such that  $\theta_j : \mathbb{R}^d \mapsto \mathbb{R} \times \mathbb{R}^{M+1}$ , which outputs  $\gamma^{(j)}(\mathbf{z})$  and  $b^{(j)}(\mathbf{z})$ .

Consequently, CRPS loss is computed in the closed form as

$$\begin{aligned} & \text{CRPS}(D_j(\cdot|\mathbf{z}; \theta_j), \mathbf{x}_j) \\ &= (2\tilde{\alpha}_j - 1)\mathbf{x}_j + (1 - 2\tilde{\alpha}_j)\gamma^{(j)}(\mathbf{z}) \\ &+ \sum_{m=1}^M b_m^{(j)}(\mathbf{z}) \left( \frac{1 - d_m^3}{3} - d_m \right. \\ &\quad \left. - \max(\tilde{\alpha}_j, d_m) + 2\max(\tilde{\alpha}_j, d_m)d_m \right), \end{aligned}$$

where

$$\begin{aligned} D_j(\tilde{\alpha}_j|\mathbf{z}; \theta_j) &= \mathbf{x}_j \\ \tilde{\alpha}_j &= \frac{\mathbf{x}_j - \gamma^{(j)}(\mathbf{z}) + \sum_{m=1}^{m_0} b_m^{(j)}(\mathbf{z})d_m}{\sum_{m=1}^{m_0} b_m^{(j)}(\mathbf{z})} \\ D_j(d_{m_0}|\mathbf{z}; \theta_j) &\leq \mathbf{x}_j \leq D_j(d_{m_0+1}|\mathbf{z}; \theta_j) \\ j &= 1, 2, \dots, p_1. \end{aligned}$$

It indicates that our objective function (3) is still computationally tractable even if we consider an infinite number of quantile levels.

### 3.3 Sampling Mechanism

To generate a synthetic sample, we first sample a latent variable from the prior distribution (the  $d$ -dimensional standard Gaussian distribution). And all continuous and discrete variables share the same sampled latent variable  $z$ . Denote  $\hat{x}_j$  as a synthetic sample of  $\mathbf{x}_j$ , for  $j = 1, \dots, p$ .

For  $j = 1, \dots, p_1$ , continuous variables, we generate a synthetic sample by inverse transform sampling. Specifically,  $\hat{x}_j = D_j(u_j|z; \theta_j)$ , where  $u_j \sim U(0, 1)$  and  $U$  is uniform distribution. For  $l = p_1 + 1, \dots, p$ , discrete variables, we use the Gumbel-Max trick Gumbel (1954) to generate a synthetic sample.  $\hat{x}_l = \arg \max_{t=1, \dots, T_l} \{\log \pi(z; \theta_l)_t + G_t\}$ , where  $G_t \sim \text{i.i.d. Gumbel}(0, 1)$ ,  $t = 1, \dots, T_l$  and  $\text{Gumbel}$  is Gumbel distribution. We discover that even when the labels of the discrete variable are highly imbalanced, the sampling based on the Gumbel-Max trick maintains the label's imbalanced ratio.

### 3.4 Calibration of Estimated CDF

To ensure that the estimated CDF is properly discretized according to the support of the variable, especially the count variable, a post-ad-hoc calibration including discretization Salimans et al. (2017) can be applied. Here, we denote the Monte Carlo approximated estimated CDF  $\hat{F}(x; \theta) := \frac{1}{B} \sum_{b=1}^B D^{-1}(x|z_b; \theta)$  for  $x \in \mathbb{R}$ , where the subscript  $j$  is omitted for brevity. Let the observed possible values set of the variable to be discretized is  $\{x^{(1)}, x^{(2)}, \dots, x^{(m)}\}$ . The calibration algorithm of the estimated CDF is shown in Algorithm 1, and an example of the calibration algorithm result is shown in Figure 1.

## 4 Experiments

In this section, to illustrate that our proposed method can capture the underlying distribution of the

---

**Algorithm 1** Calibration of Estimated CDF

---

**Input**  $\{x^{(1)}, x^{(2)}, \dots, x^{(m)}\}, \hat{F}(\cdot; \theta)$

**Output** Calibrated estimated CDF  $\hat{F}^*(\cdot; \theta)$

(1) Compute  $\hat{F}(x^{(i)} - 0.5; \theta)$  and  $\hat{F}(x^{(i)} + 0.5; \theta)$  for  $i = 1, \dots, m$ .

(2) Discretization: For  $i = 1, \dots, m$ ,

$$\begin{aligned} \hat{F}^*(x^{(i)}; \theta) &:= \hat{F}^*(x^{(i-1)}; \theta) \\ &+ \hat{F}(x^{(i)} + 0.5; \theta) - \hat{F}(x^{(i)} - 0.5; \theta), \end{aligned}$$

where  $\hat{F}^*(x^{(0)}; \theta) := 0$ .

(3) Ensure monotonicity: For  $i = 1, \dots, m - 1$ , if  $\hat{F}^*(x^{(i)}; \theta) > \hat{F}^*(x^{(i+1)}; \theta)$ ,

$$\hat{F}^*(x^{(i+1)}; \theta) := \hat{F}^*(x^{(i)}; \theta).$$

---

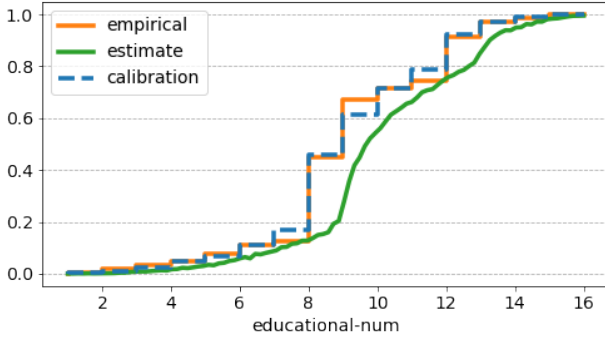


Figure 1: Calibrated estimated CDF for educational-num covariate of adult dataset. ‘estimate’ indicates  $\hat{F}(\cdot; \theta)$ , ‘calibration’ indicates  $\hat{F}^*(\cdot; \theta)$ , and ‘empirical’ indicates the empirical CDF of the observed dataset.

given dataset, we numerically show that DistVAE can generate synthetic data, which can be used as a good proxy of the original data.

## 4.1 Overview

**Dataset.** For evaluation, we consider following real tabular datasets: `covertime`, `credit`, `loan`, `adult`, `cabs`, and `kings` (see Appendix A.6 for detailed data descriptions).

**Compared models.** We compared the state-of-the-art synthesizers; CTGAN Xu et al. (2019), TVAE Xu et al. (2019), and CTAB-GAN Zhao et al. (2021). Notably, all models have the same size of the latent dimension.

## 4.2 Evaluation Metrics

To evaluate the synthetic data quality, we investigate three types of metrics: machine learning utility, statistical similarity, and privacy preservability. Note that we computed all these metrics after standardization because continuous variables have different units.

**Machine learning utility.** To evaluate the machine learning utility (MLu), we use the synthetic data as training data for three widely used machine learning algorithms: linear (logistic) regression, Random Forest, and Gradient Boosting. We average the following metrics: Mean Absolute Relative Error (MARE) for the regression and  $F_1$  for the classification problem. We choose  $F_1$  since some discrete target variables have imbalanced labels. Note that the synthetic and real training data have the same size.

To measure the MLu, the coefficient of determination  $R^2$  has been widely used Xu et al. (2019); Zhao et al. (2021); Wen et al. (2021); Kamthe et al. (2021). However, Li (2017) shows that the  $R^2$  should not be used to assess predictive performance because  $R^2$  is biased, insufficient, and misleading. Because we need to aggregate predictive performance in several different datasets, we use MARE, which is scale independent and bounded from zero to one Botchkarev (2019).

**Statistical similarity.** Next, to measure the statistical similarity between real and synthetic data, we use two statistical distances; the Kolmogorov statistic and the 1-Wasserstein distance, which measure the distance between empirical CDFs of real training data and synthetic data. The Kolmogorov statistic tests whether samples are drawn from a specific reference distribution (testing goodness of fit) Lehmann (1998). Note that we average the statistical distances across all variables.

**Privacy preservability.** Lastly, to check whether privacy is preserved in synthetic data generation, we use three metrics; *Distance to Closest Record* (DCR) Park et al. (2018); Zhao et al. (2021), *membership inference attack* Shokri et al. (2016); Choi et al. (2017); Park et al. (2018), and *attribute disclosure* Choi et al. (2017); Matwin et al. (2015).

As in Zhao et al. (2021), we define the DCR as the 5<sup>th</sup> percentiles of  $L_2$  distances between all real and synthetic samples (or between synthetic samples). Since DCR is a  $L_2$  distance-based metric, we compute DCR for only continuous variables. The higher score of DCR between the real and synthetic datasets indicates that privacy is preserved well since it implies no overlapped record between real and synthetic datasets. However, if the DCR score is too large, it indicates that the quality of the generated synthetic dataset is very poor.

The membership inference attack is evaluated ac-

cording to the steps outlined in Appendix A.7. Since we customize the membership inference attack procedure to attack a VAE-based synthesizer, only DistVAE and TVAE are assessed. Since we convert the problem of identifying the complex relationship between real and synthetic dataset members into a binary classification problem, better binary classification scores indicate that the target synthesizer is vulnerable to the membership inference attack.

Attribute disclosure occurs when attackers can reveal additional covariates of a record based on a subset of covariates that attackers already have and similar records from the synthetic dataset. In addition, classification metrics are utilized to check the degree to which attackers accurately identify additional variables. Therefore, higher attribute disclosure metrics indicate that attackers can reveal unknown variables precisely, and the target synthesizer has an increased risk of privacy leakage. Since attackers are assumed to have only a subset of covariates of a record in attribute disclosure, attribute disclosure can be considered more major privacy leakage issue.

### 4.3 Results Analysis

Table 1: Averaged machine learning utilities for synthetic datasets. Mean and standard deviation values are obtained from 10 repeated experiments.  $\uparrow$  denotes higher is better and  $\downarrow$  denotes lower is better.

Model	MARE $\downarrow$	$F_1$ $\uparrow$
CTGAN	0.321 $\pm$ 0.271	0.672 $\pm$ 0.234
TVAE	<b>0.225</b> $\pm$ 0.215	0.594 $\pm$ 0.295
CTAB-GAN	0.403 $\pm$ 0.392	0.702 $\pm$ 0.162
DistVAE( $\beta = 0.5$ )	0.349 $\pm$ 0.328	<b>0.769</b> $\pm$ 0.128
Baseline	0.150 $\pm$ 0.200	0.814 $\pm$ 0.101

**Machine learning utility.** Table 1 shows the averaged MLu for all tabular datasets, and a better synthesizer is expected to generate synthetic data which shows comparable predictive performance to that of the real training dataset (which is denoted as ‘Baseline’). DistVAE shows a competitive MARE score and outperforms other methods in  $F_1$ .

For the detailed comparison, we plot the paired (MARE,  $F_1$ ) scores for all tabular datasets and compared models in Figure 2. In Figure 2, a better score (i.e., the synthesizer having the better MLu) is indicated by a dot in the upper left corner. Figure 2 demonstrates that DistVAE consistently shows the best or at least competitive MLu across all tabular datasets.

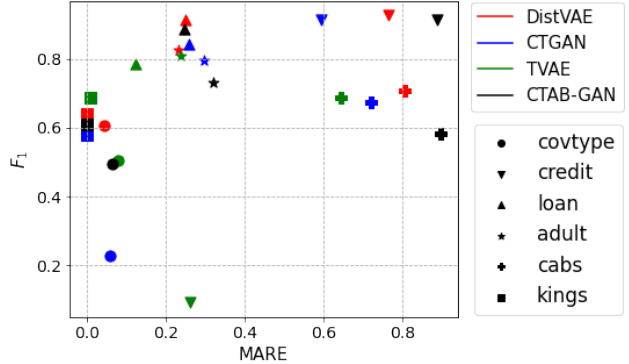


Figure 2: Machine learning utilities for compared models and real tabular datasets.

Note that TVAE shows quite a low  $F_1$  score in **credit** dataset because it fails to handle the highly imbalanced categorical target variable. See Appendix A.9 for detailed MLu scores for all tabular datasets.

Table 2: Averaged statistical similarity of synthetic datasets. K-S represents the Kolmogorov–Smirnov statistic, and 1-WD represents the 1-Wasserstein distance. Mean and standard deviation values are obtained from 10 repeated experiments. Lower is better.

(a) Continuous		
Model	K-S	1-WD
CTGAN	0.133 $\pm$ 0.106	0.087 $\pm$ 0.025
TVAE	0.196 $\pm$ 0.135	0.220 $\pm$ 0.099
CTAB-GAN	0.157 $\pm$ 0.089	0.130 $\pm$ 0.037
DistVAE( $\beta = 0.5$ )	<b>0.090</b> $\pm$ 0.065	<b>0.075</b> $\pm$ 0.026
(b) Discrete		
Model	K-S	1-WD
CTGAN	0.168 $\pm$ 0.195	0.521 $\pm$ 0.532
TVAE	0.385 $\pm$ 0.144	1.681 $\pm$ 1.668
CTAB-GAN	0.106 $\pm$ 0.083	0.412 $\pm$ 0.378
DistVAE( $\beta = 0.5$ )	<b>0.030</b> $\pm$ 0.017	<b>0.118</b> $\pm$ 0.100

**Statistical similarity.** The averaged statistical similarity is reported in Table 2. DistVAE achieves the best statistical similarity for continuous variables between real and synthetic datasets in the Kolmogorov–Smirnov statistic and 1-Wasserstein distance. It implies that the proposed distributional learning method with the CRPS loss can precisely capture the observed dataset’s underlying distribution.

For discrete variables, Table 2 indicates that Dist-

VAE outperforms in the statistical similarity performance. Note that we do not rely on the additional training technique such as *training-by-sampling* Xu et al. (2019), which causes computational burden. See Appendix A.9 for detailed statistical similarity scores for all tabular datasets.

Table 3: Privacy preservability: Averaged distance to closest record (DCR) between real and synthetic datasets (R&S) and between the same synthetic datasets (S). Mean and standard deviation values are obtained from 10 repeated experiments. Higher is better.

Model	R&S	S
CTGAN	0.426 $\pm$ 0.229	0.356 $\pm$ 0.202
TVAE	0.470 $\pm$ 0.181	0.278 $\pm$ 0.195
CTAB-GAN	0.508 $\pm$ 0.259	0.039 $\pm$ 0.073
DistVAE( $\beta = 0.5$ )	0.444 $\pm$ 0.250	0.463 $\pm$ 0.288
DistVAE( $\beta = 1$ )	0.463 $\pm$ 0.282	0.479 $\pm$ 0.310
DistVAE( $\beta = 5$ )	<b>0.517</b> $\pm$ 0.272	<b>0.511</b> $\pm$ 0.335

**Privacy preservability.** The privacy preservability of each model based on DCR scores is shown in Table 3, and we evaluate DCR scores of DistVAE with various  $\beta$  values. As  $\beta$  increases, the DCR between the real and synthetic datasets of DistVAE (R&S) increases. It implies that  $\beta$  can control the risk of privacy leakage. Also, DistVAE consistently shows the larger DCR for the synthetic dataset (S) for all  $\beta$  values. It means that DistVAE can generate more diverse synthetic samples than other methods. We find duplicated records in the synthetic dataset generated by CTAB-GAN, which results in a relatively low DCR score for the synthetic dataset (S). See Appendix A.9 for detailed DCR scores for all tabular datasets.

Table 4: Privacy preservability: Averaged membership inference attack performance. Mean and standard deviation values are obtained from 10 repeated experiments. Lower is better.

Model	Accuracy	AUC
TVAE	0.495 $\pm$ 0.019	0.495 $\pm$ 0.019
DistVAE( $\beta = 0.5$ )	0.500 $\pm$ 0.003	0.500 $\pm$ 0.003

We prepared the attack models to evaluate the membership inference attack (one per class) following the steps outlined in Section A.7. Also, the attack testing records consist of the same number of real training and test records; real training and test records have the labels of *in* and *out*, respectively. Note that the real test

records are not used to build attack models. We use gradient-boosting classifiers as attack models. Due to computational issues, the number of attack models is one (i.e.,  $C = 1$ ).

Since the target *in/out* labels are balanced and the membership inference attack is a binary classification problem, we consider accuracy and AUC (Area Under Curve) as binary classification metrics. Table 4 shows that DistVAE and TVAE attain an AUC score of 0.5, meaning that attack models can not distinguish between members of real training and test datasets, and the membership inference attack is unsuccessful. Therefore, DistVAE can generate synthetic datasets while preserving privacy regarding the membership inference attack. See Appendix A.9 for detailed membership inference attack performances for all tabular datasets.

Table 5: Privacy preservability: Averaged attribute disclosure performance with  $F_1$ , where the number of known variables is set to 5 for all tabular datasets. Mean and standard deviation values are obtained from 10 repeated experiments. Lower is better. The number in the parentheses represents the value of  $\beta$ .

Model	Number of neighbors ( $k$ )		
	1	10	100
CTGAN	0.262 $\pm$ 0.091	0.282 $\pm$ 0.087	0.275 $\pm$ 0.087
TVAE	0.437 $\pm$ 0.162	0.438 $\pm$ 0.160	0.432 $\pm$ 0.162
CTAB-GAN	<b>0.257</b> $\pm$ 0.123	0.258 $\pm$ 0.114	0.261 $\pm$ 0.111
DistVAE(0.5)	0.328 $\pm$ 0.088	0.328 $\pm$ 0.076	0.310 $\pm$ 0.072
DistVAE(1)	0.307 $\pm$ 0.073	0.313 $\pm$ 0.068	0.297 $\pm$ 0.066
DistVAE(5)	0.265 $\pm$ 0.105	<b>0.253</b> $\pm$ 0.103	<b>0.232</b> $\pm$ 0.101

We evaluate attribute disclosure based on the experiment setup of Choi et al. (2017) while varying the number of nearest neighbors in the synthetic dataset. In detail, we assume that only continuous variables are known to attackers and set the number of covariates known to the attacker as 5. Unknown discrete variables are estimated based on the majority vote of  $k$ -nearest neighbors. Note that we construct the nearest neighbors based on  $L_2$  distance. The attribute disclosure performance is measured by  $F_1$  because imbalanced discrete variables exist across all tabular datasets.

The results of attribute disclosure performance are presented in Table 5. For all numbers of neighbors ( $k$ ), the  $F_1$  score of DistVAE decreases as  $\beta$  increases, and DistVAE achieves the smallest  $F_1$  scores where  $k$  is 10 and 100. These results indicate that DistVAE can generate synthetic datasets with a low risk of attribute disclosure, and the privacy level is controlled by  $\beta$ . See Appendix A.9 for detailed attribute disclosure

performances for all tabular datasets.

### 4.3.1 Additional Study

To check the accuracy of the estimated quantile function from DistVAE, we evaluate DistVAE with the  $\alpha$ -Rate Chen et al. (2011) criterion.  $\alpha$ -Rate is defined as:

$$\alpha\text{-Rate} = \frac{1}{|I_{test}|} \sum_{i \in I_{test}} I(x_i < \hat{F}^{-1}(\alpha)), \quad (5)$$

where  $\hat{F}^{-1}(\cdot)$  is the estimated quantile function,  $\alpha \in [0, 1]$ , and  $I_{test}$  is the set of indices of test dataset.  $\alpha$ -Rate is simply the proportion of compliance samples. Inherently, the  $\alpha$ -Rate should be close to the  $\alpha$ .

Table 6: Averaged  $\alpha$ -Rate and  $|\alpha - \alpha\text{-Rate}|$  for all test datasets.

$\alpha$	0.1	0.3	0.5	0.7	0.9
$\alpha\text{-Rate}$	0.204	0.373	0.533	0.725	0.908
$ \alpha - \alpha\text{-Rate} $	0.104	0.083	0.04	0.032	0.008

We estimate quantiles for five levels (0.1, 0.3, 0.5, 0.7, 0.9) based on the estimated marginal CDFs 3 and Table 6 shows the averaged  $\alpha$ -Rate results of DistVAE across all tabular datasets. As  $\alpha$  increases from 0.1 to 0.9, the ratio of violation test samples decreases. It implies that quantiles estimated by DistVAE can be incorrect for lower quantile levels. We conjecture that extremely skewed continuous variables, such as **capital-gain** and **capital-loss** from **adult** dataset, make the quantile estimation unstable.

## 5 Conclusion and Limitations

This paper proposes a novel distributional learning method for VAE to capture the underlying distribution of the observed dataset. In this paper, distributional learning is defined as estimating the conditional CDF; hence, there is no assumption on the generative model of the VAE. Distributional learning is enabled by estimating an infinite number of conditional quantiles, which becomes computationally tractable by adopting the CRPS loss. And we show that our objective function is a proper relative to the true conditional quantile function.

Since each conditional CDF depends on a common latent variable (confounded structure), the latent variable simultaneously affects the generation process of all covariates, which makes covariates correlated in the

synthetic data generation process. However, the correlation structure of covariates can only be ‘partially’ explained by the confounded design of the latent variable because it can not account for the direct correlation structure. So, our future work is extending the decoder modeling by including the direct correlation structure between covariates.

## References

- Akrami, H., Joshi, A. A., Aydöre, S., and Leahy, R. M. Addressing variance shrinkage in variational autoencoders using quantile regression. *ArXiv*, abs/2010.09042, 2020.
- Blei, D. M., Kucukelbir, A., and McAuliffe, J. D. Variational inference: A review for statisticians. *Journal of the American Statistical Association*, 112:859 – 877, 2016.
- Botchkarev, A. A new typology design of performance metrics to measure errors in machine learning regression algorithms. *Interdisciplinary Journal of Information, Knowledge, and Management*, 2019.
- Burda, Y., Grosse, R. B., and Salakhutdinov, R. Importance weighted autoencoders. *CoRR*, abs/1509.00519, 2015.
- Chen, C. W. S., Gerlach, R. H., Hwang, B. B. K., and McAleer, M. Forecasting value-at-risk using non-linear regression quantiles and the intra-day range. 2011.
- Choi, E., Biswal, S., Malin, B. A., Duke, J. D., Stewart, W. F., and Sun, J. Generating multi-label discrete patient records using generative adversarial networks. In *Machine Learning in Health Care*, 2017.
- Gasthaus, J., Benidis, K., Wang, Y., Rangapuram, S. S., Salinas, D., Flunkert, V., and Januschowski, T. Probabilistic forecasting with spline quantile function rnns. In *The 22nd international conference on artificial intelligence and statistics*, pp. 1901–1910. PMLR, 2019.
- Gneiting, T. and Raftery, A. E. Strictly proper scoring rules, prediction, and estimation. *Journal of the American Statistical Association*, 102:359 – 378, 2007.
- Goodfellow, I. J., Pouget-Abadie, J., Mirza, M., Xu, B., Warde-Farley, D., Ozair, S., Courville, A. C., and Bengio, Y. Generative adversarial nets. In *NIPS*, 2014.

- Gumbel, E. J. *Statistical theory of extreme values and some practical applications: a series of lectures*, volume 33. US Government Printing Office, 1954.
- Higgins, I., Matthey, L., Pal, A., Burgess, C., Glorot, X., Botvinick, M., Mohamed, S., and Lerchner, A. beta-vae: Learning basic visual concepts with a constrained variational framework. 2016.
- Kamthe, S., Assefa, S. A., and Deisenroth, M. P. Copula flows for synthetic data generation. *ArXiv*, abs/2101.00598, 2021.
- Karras, T., Laine, S., and Aila, T. A style-based generator architecture for generative adversarial networks. *2019 IEEE/CVF Conference on Computer Vision and Pattern Recognition (CVPR)*, pp. 4396–4405, 2018.
- Kingma, D. P. and Welling, M. Auto-encoding variational bayes. *CoRR*, abs/1312.6114, 2013.
- Kingma, D. P., Salimans, T., and Welling, M. Improved variational inference with inverse autoregressive flow. *ArXiv*, abs/1606.04934, 2016.
- Larsen, A. B. L., Sønderby, S. K., Larochelle, H., and Winther, O. Autoencoding beyond pixels using a learned similarity metric. *ArXiv*, abs/1512.09300, 2015.
- Lehmann, E. L. Elements of large-sample theory. 1998.
- Li, J. Assessing the accuracy of predictive models for numerical data: Not  $r$  nor  $r^2$ , why not? then what? *PLoS ONE*, 12, 2017.
- Lucas, J., Tucker, G., Grosse, R. B., and Norouzi, M. Don’t blame the elbo! a linear vae perspective on posterior collapse. In *Advances in Neural Information Processing Systems*, pp. 9408–9418, 2019.
- Matheson, J. E. and Winkler, R. L. Scoring rules for continuous probability distributions. *Management Science*, 22:1087–1096, 1976.
- Matwin, S., Nin, J., Sehatkar, M., and Szapiro, T. A review of attribute disclosure control. In *Advanced Research in Data Privacy*, 2015.
- Moon, S., Jeon, J.-J., Lee, J. E. H., and Kim, Y. Learning multiple quantiles with neural networks. *Journal of Computational and Graphical Statistics*, 30:1238 – 1248, 2021.
- Munjal, P., Paul, A., and Krishnan, N. C. Implicit discriminator in variational autoencoder. *2020 International Joint Conference on Neural Networks (IJCNN)*, pp. 1–8, 2019.
- Park, N., Mohammadi, M., Gorde, K., Jajodia, S., Park, H., and Kim, Y. Data synthesis based on generative adversarial networks. *Proc. VLDB Endow.*, 11:1071–1083, 2018.
- Rosca, M., Lakshminarayanan, B., Warde-Farley, D., and Mohamed, S. Variational approaches for auto-encoding generative adversarial networks. *ArXiv*, abs/1706.04987, 2017.
- Salimans, T., Karpathy, A., Chen, X., and Kingma, D. P. Pixelcnn++: Improving the pixelcnn with discretized logistic mixture likelihood and other modifications. *ArXiv*, abs/1701.05517, 2017.
- Shokri, R., Stronati, M., Song, C., and Shmatikov, V. Membership inference attacks against machine learning models. *2017 IEEE Symposium on Security and Privacy (SP)*, pp. 3–18, 2016.
- Takahashi, H., Iwata, T., Yamanaka, Y., Yamada, M., and Yagi, S. Student-t variational autoencoder for robust density estimation. In *International Joint Conference on Artificial Intelligence*, 2018.
- Wang, W., Gan, Z., Xu, H., Zhang, R., Wang, G., Shen, D., Chen, C., and Carin, L. Topic-guided variational autoencoders for text generation. *arXiv preprint arXiv:1903.07137*, 2019.
- Wen, B., Colon, L. O., Subbalakshmi, K., and Chandramouli, R. Causal-tgan: Generating tabular data using causal generative adversarial networks. *ArXiv*, abs/2104.10680, 2021.
- Xu, L., Skoularidou, M., Cuesta-Infante, A., and Veeramachaneni, K. Modeling tabular data using conditional gan. *ArXiv*, abs/1907.00503, 2019.
- Yu, K. and Moyeed, R. Bayesian quantile regression. *Statistics & Probability Letters*, 54:437–447, 2001.
- Zhao, Z., Kunar, A., van der Scheer, H., Birke, R., and Chen, L. Y. Ctab-gan: Effective table data synthesizing. *ArXiv*, abs/2102.08369, 2021.

## A Appendix

### A.1 Derivation of ELBO

$$\begin{aligned}
& \log p(\mathbf{x}; \theta, \beta) \\
= & \log \int p(\mathbf{x}|\mathbf{z}; \theta, \beta) p(\mathbf{z}) d\mathbf{z} \\
= & \log \sum_{k=1}^K p(\alpha_k) \int p(\mathbf{x}|\mathbf{z}, \alpha_k; \theta, \beta) p(\mathbf{z}) d\mathbf{z} \\
= & \log \sum_{k=1}^K p(\alpha_k) \int p(\mathbf{x}|\mathbf{z}, \alpha_k; \theta, \beta) \frac{p(\mathbf{z})}{q(\mathbf{z}|\mathbf{x}; \phi)} q(\mathbf{z}|\mathbf{x}; \phi) d\mathbf{z} \\
\geq & \sum_{k=1}^K p(\alpha_k) \int q(\mathbf{z}|\mathbf{x}; \phi) \log \left( p(\mathbf{x}|\mathbf{z}, \alpha_k; \theta, \beta) \frac{p(\mathbf{z})}{q(\mathbf{z}|\mathbf{x}; \phi)} \right) d\mathbf{z} \\
= & \frac{1}{K} \sum_{k=1}^K \mathbb{E}_{q(\mathbf{z}|\mathbf{x}; \phi)} [\log p(\mathbf{x}|\mathbf{z}, \alpha_k; \theta, \beta)] - \mathcal{KL}(q(\mathbf{z}|\mathbf{x}; \phi) \| p(\mathbf{z})) \\
= & \frac{1}{K} \sum_{k=1}^K \mathbb{E}_{q(\mathbf{z}|\mathbf{x}; \phi)} \left[ \sum_{j=1}^{p_1} \log p(\mathbf{x}_j|\mathbf{z}, \alpha_k; \theta_j, \beta) + \sum_{l=p_1+1}^p \log p(\mathbf{x}_l|\mathbf{z}, \alpha_k; \theta_j, \beta) \right] - \mathcal{KL}(q(\mathbf{z}|\mathbf{x}; \phi) \| p(\mathbf{z})) \\
= & \frac{1}{K} \sum_{k=1}^K \mathbb{E}_{q(\mathbf{z}|\mathbf{x}; \phi)} \left[ \sum_{j=1}^{p_1} \log p(\mathbf{x}_j|\mathbf{z}, \alpha_k; \theta_j, \beta) \right] + \mathbb{E}_{q(\mathbf{z}|\mathbf{x}; \phi)} \left[ \sum_{l=p_1+1}^p \log p(\mathbf{x}_l|\mathbf{z}; \theta_j, \beta) \right] - \mathcal{KL}(q(\mathbf{z}|\mathbf{x}; \phi) \| p(\mathbf{z})) \\
= & \mathbb{E}_{q(\mathbf{z}|\mathbf{x}; \phi)} \left[ \sum_{j=1}^{p_1} \frac{1}{K} \sum_{k=1}^K \log \frac{\alpha_k(1 - \alpha_k)}{\beta} - \rho_{\alpha_k} \left( \frac{\mathbf{x}_j - D_j(\alpha_k|\mathbf{z}, \theta_j)}{\beta} \right) \right] \\
& + \mathbb{E}_{q(\mathbf{z}|\mathbf{x}; \phi)} \left[ \sum_{l=p_1+1}^p \sum_{t=1}^{T_l} I(\mathbf{x}_l = t) \cdot \log \pi(\mathbf{z}; \theta_l)_t \right] - \mathcal{KL}(q(\mathbf{z}|\mathbf{x}; \phi) \| p(\mathbf{z})) \\
= & \sum_{j=1}^{p_1} \mathbb{E}_{q(\mathbf{z}|\mathbf{x}; \phi)} \left[ -\frac{1}{2 \cdot \beta} \cdot \frac{1}{K} \sum_{k=1}^K 2 \cdot \rho_{\alpha_k} \left( \mathbf{x}_j - D_j(\alpha_k|\mathbf{z}, \theta_j) \right) \right] + \frac{p_1}{K} \sum_{k=1}^K \log \alpha_k(1 - \alpha_k) - p_1 \cdot \log \beta \\
& + \sum_{l=p_1+1}^p \mathbb{E}_{q(\mathbf{z}|\mathbf{x}; \phi)} \left[ \sum_{t=1}^{T_l} I(\mathbf{x}_l = t) \cdot \log \pi(\mathbf{z}; \theta_l)_t \right] - \mathcal{KL}(q(\mathbf{z}|\mathbf{x}; \phi) \| p(\mathbf{z})) \\
= & -\frac{1}{\beta} \left( \sum_{j=1}^{p_1} \mathbb{E}_{q(\mathbf{z}|\mathbf{x}; \phi)} \left[ \frac{1}{2 \cdot K} \sum_{k=1}^K 2 \cdot \rho_{\alpha_k} \left( \mathbf{x}_j - D_j(\alpha_k|\mathbf{z}, \theta_j) \right) \right] - \beta p_1 \frac{1}{K} \sum_{k=1}^K \log \alpha_k(1 - \alpha_k) + \beta p_1 \log \beta \right. \\
& \left. - \beta \cdot \sum_{l=p_1+1}^p \mathbb{E}_{q(\mathbf{z}|\mathbf{x}; \phi)} \left[ \sum_{t=1}^{T_l} I(\mathbf{x}_l = t) \cdot \log \pi(\mathbf{z}; \theta_l)_t \right] + \beta \cdot \mathcal{KL}(q(\mathbf{z}|\mathbf{x}; \phi) \| p(\mathbf{z})) \right),
\end{aligned}$$

by Jensen's inequality.

## A.2 Model Misspecification Error

Let  $g(\mathbf{x})$  be the continuous ground-truth density function of  $\mathbf{x}$  where  $\mathbf{x} \sim i.i.d. g(\mathbf{x})$ , and we consider a parametric generative model  $\{p(\cdot; \theta) : \theta \in \Omega\}$ . The VAE framework is based on the Maximum Likelihood Estimation (MLE) objective

$$\max_{p \in \{p(\cdot; \theta) : \theta \in \Omega\}} \int g(\mathbf{x}) \log p(\mathbf{x}) d\mathbf{x}, \quad (6)$$

and the model misspecification error  $\mathcal{KL}(g\|p(\cdot|\theta))$  in MLE is written as

$$\mathcal{KL}(g\|p(\cdot; \theta)) = \int g(\mathbf{x}) \log g(\mathbf{x}) d\mathbf{x} - \int g(\mathbf{x}) \log p(\mathbf{x}; \theta) d\mathbf{x}.$$

**Assumption 2.** For  $\forall \theta \in \Omega$ ,  $p(\cdot; \theta)$  is a continuous distribution and absolutely continuous with respect to  $g$ .

The generative distribution of Gaussian VAE is written as

$$p(\mathbf{x}; \theta) = \int \mathcal{N}(\mathbf{x}|D(\mathbf{z}; \theta), \beta \cdot I) \cdot \mathcal{N}(\mathbf{z}|0, I) d\mathbf{z}, \quad (7)$$

and the VAE model is trained by maximizing the lower bound of (6). Note that the generative distribution is constrained in the form of marginalization of the product of two Gaussian distributions, as mentioned in Section 1. It implies that we are prone to fit the incorrect family of densities (misspecified generative distributional family). Consequently, we obtain the worse estimation of  $\theta$  according to the criterion (6), since  $\mathcal{KL}(g\|p(\cdot; \theta)) \gg 0$  and  $\int g(\mathbf{x}) \log g(\mathbf{x}) d\mathbf{x}$  is fixed.

In the existing methods of Gaussian VAE, the parametric model is assumed as

$$\begin{aligned} \mathcal{S}_1 &= \left\{ p(\cdot; \theta) \quad : \quad \Pr(\mathbf{x} \leq x; \theta) = \int_{-\infty}^x p(t; \theta) dt \right. \\ &=: F(x; \theta) = \int F(x|\mathbf{z}; \theta) p(\mathbf{z}) d\mathbf{z} = \int \prod_{j=1}^p F_j(x_j|\mathbf{z}; \theta_j) p(\mathbf{z}) d\mathbf{z} = \left. \int \prod_{j=1}^p \Phi(x_j|\mathbf{z}; \theta_j) p(\mathbf{z}) d\mathbf{z} \right\} \end{aligned}$$

where  $p(\mathbf{z}) = \mathcal{N}(\mathbf{z}|0, I)$ ,  $\Phi(\cdot|\mathbf{z}; \theta_j)$  is CDF of  $\mathcal{N}(\cdot|D(\mathbf{z}; \theta_j), \beta)$ , and  $D(\cdot; \theta_j) : \mathbb{R}^d \mapsto \mathbb{R}$  is a neural network parameterized with  $\theta_j$  for  $j = 1, \dots, p$ .

On the other hand, the parametric model of our DistVAE is defined as

$$\begin{aligned} \mathcal{S}_2 &= \left\{ p(\cdot; \theta) \quad : \quad \Pr(\mathbf{x} \leq x; \theta) = \int_{-\infty}^x p(t; \theta) dt \right. \\ &=: F(x; \theta) = \int F(x|\mathbf{z}, \theta) p(\mathbf{z}) d\mathbf{z} = \left. \int \prod_{j=1}^p F_j(x_j|\mathbf{z}; \theta_j) p(\mathbf{z}) d\mathbf{z} \right\} \end{aligned}$$

where  $p(\mathbf{z}) = \mathcal{N}(\mathbf{z}|0, I)$ ,  $F_j(\cdot|\mathbf{z}; \theta_j) : \mathbb{R} \times \mathbb{R}^d \mapsto [0, 1]$  is the monotone increasing function and CDF of  $\mathbf{x}_j$ .

Since DistVAE directly estimates the conditional CDF without distributional assumption,  $\mathcal{S}_1 \subset \mathcal{S}_2$ . Therefore, the next Proposition 4 guarantees that DistVAE produces a better generative model in terms of (6) when the ELBO is tight.

**Proposition 4** (Lower Model Misspecification Error.). Let  $p(\mathbf{x}; \hat{\theta}_1) = \arg \max_{p \in \mathcal{S}_1} \int g(\mathbf{x}) \log p(\mathbf{x}) d\mathbf{x}$  and  $p(\mathbf{x}; \hat{\theta}_2) = \arg \max_{p \in \mathcal{S}_2} \int g(\mathbf{x}) \log p(\mathbf{x}) d\mathbf{x}$ , where  $\mathcal{S}_1 = \{p(\cdot; \theta) : \theta \in \Omega_1\}$  and  $\mathcal{S}_2 = \{p(\cdot; \theta) : \theta \in \Omega_2\}$ . If  $\mathcal{S}_1 \subset \mathcal{S}_2$ , then,

$$\mathcal{KL}(g\|p(\cdot; \hat{\theta}_1)) \geq \mathcal{KL}(g\|p(\cdot; \hat{\theta}_2)).$$

*Proof.* Since  $\mathcal{S}_1 \subset \mathcal{S}_2$ ,

$$\max_{p \in \mathcal{S}_1} \int g(\mathbf{x}) \log p(\mathbf{x}) d\mathbf{x} \leq \max_{p \in \mathcal{S}_2} \int g(\mathbf{x}) \log p(\mathbf{x}) d\mathbf{x}.$$

Therefore,

$$\begin{aligned} \mathcal{KL}(g \| p(\cdot; \hat{\theta}_1)) &= \int g(\mathbf{x}) \log g(\mathbf{x}) d\mathbf{x} - \int g(\mathbf{x}) \log p(\mathbf{x}; \hat{\theta}_1) d\mathbf{x} \\ &\geq \int g(\mathbf{x}) \log g(\mathbf{x}) d\mathbf{x} - \int g(\mathbf{x}) \log p(\mathbf{x}; \hat{\theta}_2) d\mathbf{x} \\ &= \mathcal{KL}(g \| p(\cdot; \hat{\theta}_2)). \end{aligned}$$

□

### A.3 Proof of Proposition 1

*Proof.* Suppose that  $\int_0^1 \mathbb{E}_{q(\mathbf{z}|\mathbf{x};\phi)} \left| 2 \cdot \rho_{\alpha} \left( \mathbf{x}_j - D_j(\alpha|\mathbf{z}, \theta_j) \right) \right| d\alpha < \infty$ , for  $j = 1, \dots, p_1$ .

$$\begin{aligned} \mathbb{E}_{q(\mathbf{z}|\mathbf{x};\phi)} \left[ \frac{1}{K} \sum_{k=1}^K 2 \cdot \rho_{\alpha_k} \left( \mathbf{x}_j - D_j(\alpha_k|\mathbf{z}, \theta_j) \right) \right] &= \frac{1}{K} \sum_{k=1}^K h(\alpha_k|\mathbf{x}) \\ &= \sum_{k=1}^K h(\alpha_k|\mathbf{x}) \cdot (\alpha_k - \alpha_{k-1}), \end{aligned}$$

where  $\alpha_0 := 0$  and we denote  $\mathbb{E}_{q(\mathbf{z}|\mathbf{x};\phi)} \left[ 2 \cdot \rho_{\alpha_k} \left( \mathbf{x}_j - D_j(\alpha_k|\mathbf{z}, \theta_j) \right) \right]$  as  $h(\alpha_k|\mathbf{x})$  for simplicity of the notation.

Since  $\alpha_k \in [\alpha_{k-1}, \alpha_k]$  and  $h(\cdot|\mathbf{x}) : [0, 1] \mapsto \mathbb{R}$  is a continuous function for any  $\mathbf{x} \in \mathcal{X}$ ,

$$\begin{aligned} \lim_{K \rightarrow \infty} \mathbb{E}_{q(\mathbf{z}|\mathbf{x};\phi)} \left[ \frac{1}{K} \sum_{k=1}^K 2 \cdot \rho_{\alpha_k} \left( \mathbf{x}_j - D_j(\alpha_k|\mathbf{z}, \theta_j) \right) \right] &= \lim_{K \rightarrow \infty} \sum_{k=1}^K h(\alpha_k|\mathbf{x}) \cdot (\alpha_k - \alpha_{k-1}) \\ &= \int_0^1 h(\alpha|\mathbf{x}) d\alpha \\ &= \int_0^1 \mathbb{E}_{q(\mathbf{z}|\mathbf{x};\phi)} \left[ 2 \cdot \rho_{\alpha} \left( \mathbf{x}_j - D_j(\alpha|\mathbf{z}, \theta_j) \right) \right] d\alpha \\ &= \mathbb{E}_{q(\mathbf{z}|\mathbf{x};\phi)} \left[ \int_0^1 2 \cdot \rho_{\alpha} \left( \mathbf{x}_j - D_j(\alpha|\mathbf{z}, \theta_j) \right) d\alpha \right], \end{aligned}$$

by the definition of the Riemann integral and the Fubini-Tonelli theorem.

□

#### A.4 Proof of Proposition 2

*Proof.* By Assumption 1,  $p(\mathbf{z}) = q(\mathbf{z}; \phi)$ , where  $q(\mathbf{z}; \phi) = \int q(\mathbf{z}|\mathbf{x}; \phi)q(\mathbf{x})d\mathbf{x}$ . For  $j = 1, \dots, p_1$  and  $\alpha \in (0, 1)$ ,

$$\begin{aligned}
& \mathbb{E}_{q(\mathbf{x})}\mathbb{E}_{q(\mathbf{z}|\mathbf{x}; \phi)}[\rho_\alpha(\mathbf{x}_j - D_j(\alpha|\mathbf{z}))] \\
&= \mathbb{E}_{q(\mathbf{x})}\mathbb{E}_{q(\mathbf{z}|\mathbf{x}; \phi)}\left[\left(\alpha - I(\mathbf{x}_j - D_j(\alpha|\mathbf{z}))\right)\left(\mathbf{x}_j - D_j(\alpha|\mathbf{z})\right)\right] \\
&= \alpha \cdot \mathbb{E}_{q_j(\mathbf{x}_j)}[\mathbf{x}_j] - \alpha \cdot \mathbb{E}_{q(\mathbf{z}; \phi)}[D_j(\alpha|\mathbf{z})] - \int q(\mathbf{x})q(\mathbf{z}|\mathbf{x}; \phi)\left[I(\mathbf{x}_j - D_j(\alpha|\mathbf{z}))\left(\mathbf{x}_j - D_j(\alpha|\mathbf{z})\right)\right]d\mathbf{x}d\mathbf{z} \\
&= \alpha \cdot \mathbb{E}_{q_j(\mathbf{x}_j)}[\mathbf{x}_j] - \alpha \cdot \mathbb{E}_{q(\mathbf{z}; \phi)}[D_j(\alpha|\mathbf{z})] - \int p(\mathbf{z})p(\mathbf{x}|\mathbf{z})\left[I(\mathbf{x}_j - D_j(\alpha|\mathbf{z}))\left(\mathbf{x} - D_j(\alpha|\mathbf{z})\right)\right]d\mathbf{x}d\mathbf{z} \\
&= \alpha \cdot \mathbb{E}_{q_j(\mathbf{x}_j)}[\mathbf{x}_j] - \alpha \cdot \mathbb{E}_{q(\mathbf{z}; \phi)}[D_j(\alpha|\mathbf{z})] - \int p(\mathbf{z})p_j(\mathbf{x}_j|\mathbf{z})\left[I(\mathbf{x}_j - D_j(\alpha|\mathbf{z}))\left(\mathbf{x}_j - D_j(\alpha|\mathbf{z})\right)\right]d\mathbf{x}_jd\mathbf{z} \\
&= \alpha \cdot \mathbb{E}_{q_j(\mathbf{x}_j)}[\mathbf{x}_j] - \alpha \cdot \mathbb{E}_{q(\mathbf{z}; \phi)}[D_j(\alpha|\mathbf{z})] + \mathbb{E}_{p(\mathbf{z})}\int_{-\infty}^{D_j(\alpha|\mathbf{z})}(-\mathbf{x}_j + D_j(\alpha|\mathbf{z}))dF_j(\mathbf{x}_j|\mathbf{z}) \\
&= \alpha \cdot \mathbb{E}_{q_j(\mathbf{x}_j)}[\mathbf{x}_j] + \mathbb{E}_{p(\mathbf{z})}\left[\underbrace{-\alpha \cdot D_j(\alpha|\mathbf{z}) - \int_{-\infty}^{D_j(\alpha|\mathbf{z})}\mathbf{x}_jdF_j(\mathbf{x}_j|\mathbf{z}) + D_j(\alpha|\mathbf{z})F_j(D_j(\alpha|\mathbf{z})|\mathbf{z})}_{(*)}\right],
\end{aligned}$$

where  $q_j(\mathbf{x}_j)$ ,  $p_j(\mathbf{x}_j|\mathbf{z})$ , and  $F_j(\mathbf{x}_j|\mathbf{z})$  are marginalized distributions of  $q(\mathbf{x})$ ,  $p(\mathbf{x}|\mathbf{z})$ , and  $F(\mathbf{x}|\mathbf{z})$  with respect to  $(\mathbf{x}_1, \dots, \mathbf{x}_{j-1}, \mathbf{x}_{j+1}, \dots, \mathbf{x}_p)$ , respectively.

For all  $\mathbf{z} \in \mathbb{R}^d$ ,

$$\begin{aligned}
& \frac{\partial}{\partial D_j(\alpha|\mathbf{z})} (*) \\
&= -\alpha - D_j(\alpha|\mathbf{z})\frac{\partial F_j(D_j(\alpha|\mathbf{z})|\mathbf{z})}{\partial D_j(\alpha|\mathbf{z})} + F_j(D_j(\alpha|\mathbf{z})|\mathbf{z}) + D_j(\alpha|\mathbf{z})\frac{\partial F_j(D_j(\alpha|\mathbf{z})|\mathbf{z})}{\partial D_j(\alpha|\mathbf{z})} \\
&= F_j(D_j(\alpha|\mathbf{z})|\mathbf{z}) - \alpha.
\end{aligned}$$

Therefore,  $(*)$  is minimized when  $D_j(\alpha|\mathbf{z}) = D_j^*(\alpha|\mathbf{z})$ . Note that  $D_j^*(\alpha|\mathbf{z})$  is the true conditional  $\alpha$ -quantile with respect to the true conditional CDF  $F_j(\mathbf{x}_j|\mathbf{z})$ . It implies that, under Assumption 1, for  $\alpha \in (0, 1)$ ,

$$\begin{aligned}
\mathcal{S}_\alpha(D_j, D_j^*) &= \mathbb{E}_{q(\mathbf{x})}\mathbb{E}_{q(\mathbf{z}|\mathbf{x}; \phi)}[\rho_\alpha(\mathbf{x}_j - D_j(\alpha|\mathbf{z}))] \\
&\geq \min_{D \in \mathcal{D}} \mathbb{E}_{q(\mathbf{x})}\mathbb{E}_{q(\mathbf{z}|\mathbf{x}; \phi)}[\rho_\alpha(\mathbf{x}_j - D_j(\alpha|\mathbf{z}))] \\
&= \min_{D \in \mathcal{D}} \mathbb{E}_{p(\mathbf{z})}\mathbb{E}_{p(\mathbf{x}|\mathbf{z})}[\rho_\alpha(\mathbf{x}_j - D_j(\alpha|\mathbf{z}))] \\
&= \mathbb{E}_{p(\mathbf{z})}\left\{\min_{D \in \mathcal{D}} \mathbb{E}_{p(\mathbf{x}|\mathbf{z})}[\rho_\alpha(\mathbf{x}_j - D_j(\alpha|\mathbf{z}))]\right\} \\
&= \mathbb{E}_{p(\mathbf{z})}\mathbb{E}_{p(\mathbf{x}|\mathbf{z})}[\rho_\alpha(\mathbf{x}_j - D_j^*(\alpha|\mathbf{z}))] \\
&= \mathcal{S}_\alpha(D_j^*, D_j^*),
\end{aligned} \tag{8}$$

and

$$\mathbb{E}_{q(\mathbf{x})}\mathbb{E}_{q(\mathbf{z}|\mathbf{x}; \phi)}[\rho_\alpha(\mathbf{x}_j - D_j^*(\alpha|\mathbf{z}))] = \min_{D_j \in \mathcal{D}_j} \mathcal{S}_\alpha(D_j, D_j^*).$$

Since  $\mathbb{E}_{q(\mathbf{x})}\mathbb{E}_{q(\mathbf{z}|\mathbf{x}; \phi)}\left[\int_0^1 |\rho_\alpha(\mathbf{x}_j - D_j(\alpha|\mathbf{z}))|d\alpha\right] < \infty$ ,

$$\begin{aligned}
\mathcal{S}(D_j, D_j^*) &= \mathbb{E}_{q(\mathbf{x})}\mathbb{E}_{q(\mathbf{z}|\mathbf{x}; \phi)}\left[\int_0^1 \rho_\alpha(\mathbf{x}_j - D_j(\alpha|\mathbf{z}))d\alpha\right] \\
&= \int_0^1 \mathbb{E}_{q(\mathbf{x})}\mathbb{E}_{q(\mathbf{z}|\mathbf{x}; \phi)}[\rho_\alpha(\mathbf{x}_j - D_j(\alpha|\mathbf{z}))]d\alpha = \int_0^1 \mathcal{S}_\alpha(D_j, D_j^*)d\alpha,
\end{aligned}$$

by the Fubini-Tonelli theorem. Therefore, since (8) holds for all  $\alpha \in (0, 1)$ ,

$$\begin{aligned}\mathcal{S}(D_j, D_j^*) - \mathcal{S}(D_j^*, D_j^*) &= \int_0^1 \mathcal{S}_\alpha(D_j, D_j^*) - \mathcal{S}_\alpha(D_j^*, D_j^*) d\alpha \\ &\geq 0,\end{aligned}$$

and the scoring rule  $\mathcal{S}$  is proper relative to  $D_j^*$ . □

### A.5 Proof of Proposition 3

*Proof.* For  $j = 1, 2, \dots, p_1$ , denote  $\mathbf{x}_{-j}$  as  $\mathbf{x}$  without  $\mathbf{x}_j$  where  $\mathbf{x}_{-j} \in \mathcal{X}_{-j}$ .

$$\begin{aligned}F_j(x_j) &= \int_{-\infty}^{x_j} q_j(\mathbf{x}_j) d\mathbf{x}_j \\ &= \int_{-\infty}^{x_j} \int_{\mathcal{X}_{-j}} q(\mathbf{x}) d\mathbf{x}_{-j} d\mathbf{x}_j \\ &= \int_{-\infty}^{x_j} \int_{\mathcal{X}_{-j}} \int_{\mathbb{R}^d} p(\mathbf{x}|\mathbf{z}) p(\mathbf{z}) d\mathbf{z} d\mathbf{x}_{-j} d\mathbf{x}_j \\ &= \int_{\mathbb{R}^d} \int_{-\infty}^{x_j} \int_{\mathcal{X}_{-j}} p(\mathbf{x}|\mathbf{z}) p(\mathbf{z}) d\mathbf{x}_{-j} d\mathbf{x}_j d\mathbf{z} \\ &= \int_{\mathbb{R}^d} \int_{-\infty}^{x_j} p_j(\mathbf{x}_j|\mathbf{z}) p(\mathbf{z}) d\mathbf{x}_j d\mathbf{z} \\ &= \int_{\mathbb{R}^d} F_j(x_j|\mathbf{z}) p(\mathbf{z}) d\mathbf{z} \\ &= \int_{\mathbb{R}^d} D_j^{-1}(x_j|\mathbf{z}) p(\mathbf{z}) d\mathbf{z},\end{aligned}$$

by the Fubini-Tonelli theorem such that  $\int_{\mathcal{X}} \int_{\mathbb{R}^d} |p(\mathbf{x}|\mathbf{z}; \theta) p(\mathbf{z})| d\mathbf{z} d\mathbf{x} < \infty$ , where  $q_j(\mathbf{x}_j)$ ,  $p_j(\mathbf{x}_j|\mathbf{z})$ , and  $F_j(\mathbf{x}_j|\mathbf{z})$  are marginalized distributions of  $q(\mathbf{x})$ ,  $p(\mathbf{x}|\mathbf{z})$ , and  $F(\mathbf{x}|\mathbf{z})$  with respect to  $(\mathbf{x}_1, \dots, \mathbf{x}_{j-1}, \mathbf{x}_{j+1}, \dots, \mathbf{x}_p)$ , respectively. □

## A.6 Dataset Descriptions

### Websites

- coverytype: <https://www.kaggle.com/datasets/uciml/forest-cover-type-dataset>
- credit: <https://www.kaggle.com/c/home-credit-default-risk>
- loan: <https://www.kaggle.com/datasets/teertha/personal-loan-modeling>
- adult: <https://www.kaggle.com/datasets/uciml/adult-census-income>
- cabs: <https://www.kaggle.com/datasets/arashnic/taxi-pricing-with-mobility-analytics?select=test.csv>
- kings: <https://www.kaggle.com/datasets/harlfoxem/housesalesprediction>

Table 7: Description of datasets. The notations #C and #D represent the number of continuous and discrete variables.

Dataset	Train/Test Split	Regression Target	Classification Target	#C	#D
coverytype	45k/5k	Elevation	Cover_Type	10	1
credit	45k/5k	AMT_CREDIT	TARGET	10	9
loan	4k/1k	Age	Personal Loan	5	6
adult	40k/5k	age	income	5	9
cabs	40k/1k	Trip_Distance	Surge_Pricing_Type	6	7
kings	20k/1k	long	condition	11	7

## A.7 Membership Inference Attack

Park et al. (2018) propose the customized *membership inference attack* method of Shokri et al. (2016) to attack the GAN-based synthesizer. Similarly, we propose the customized membership inference attack method of Shokri et al. (2016) to attack the VAE-based synthesizer.

**Assumption 3** (Shokri et al. (2016)). *In the membership inference attack, the attacker attacks the target model under the following assumptions:*

- (A1) *The attacker is only allowed for black-box access where the attacker can only supply inputs to the model and receive the model’s output(s).*
- (A2) *The attacker can obtain as many outputs as they want from a target model to attack.*
- (A3) *The real and synthetic datasets should not have common records.*
- (A4) *The attacker knows the algorithm and architecture of the target model.*

Denote  $D_{train}^*$  and  $D_{test}^*$  as the real training and test datasets. Under Assumption 3, the overall steps of the membership inference attack are outlined below:

1. Generate shadow training and test datasets  $D_{train}^{(i)}, D_{test}^{(i)}, i = 1, \dots, C$  from  $M^*$  by (A1), where  $M^*$  is the model attacker wants to attack. By (A2), the attacker is allowed for obtaining shadow datasets such as  $|D_{train}^{(i)}| = |D_{train}^*|$  and  $D_{train}^{(i)} \cap D_{test}^{(j)} = \emptyset$ , for  $i = 1, \dots, C$ . Under (A3),  $D_{train}^{(i)} \cap D_{train}^* = \emptyset$ , for  $i = 1, \dots, C$ .
2. Train shadow models  $M_1, \dots, M_C$  under (A4), i.e. each shadow model is trained in a similar way to the target model  $M^*$ .

3. For  $i = 1, \dots, C$ ,
  - (a) Obtain representation vectors  $\mathbf{z}$  from the encoder of  $M_i$  with the input of  $D_{train}^{(i)}$ . Then, attacking training records are  $(\mathbf{y}, \mathbf{z}, in)$ .
  - (b) Obtain representation vectors  $\mathbf{z}$  from the encoder of  $M_i$  with the input of  $D_{test}^{(i)}$ . Then, attacking training records are  $(\mathbf{y}, \mathbf{z}, out)$ .

where  $\mathbf{y}$  is the labels of shadow dataset records. And we assume that  $\mathbf{y}$  consists of the MLU classification target.

4. Merge all attack training records,  $(\mathbf{y}, \mathbf{z}, in/out)$ .
5. For each class of  $\mathbf{y}$ , train *attack model* which is a binary classification model which classifies *in/out* based on the representation vectors  $\mathbf{z}$ .
6. Now it is ready to attack.

Note that we use the representation vector of VAE instead of the output of the GAN discriminator Park et al. (2018).

## A.8 Experimental Settings

We run all experiments using Geforce RTX 3090 GPU, and our experimental codes are all available with `pytorch`.

Table 8: Hyper-parameter settings for tabular dataset experiments.

Model	epochs	batch size	learning rate	$\beta$ (or decoder std range)	$d$	$M$
CTGAN	300	500	0.0002	-	2	-
TVAE	200	256	0.005	[0.1, 1]	2	-
CTAB-GAN	150	500	0.0002	-	2	-
DistVAE	100	256	0.001	0.5	2	10

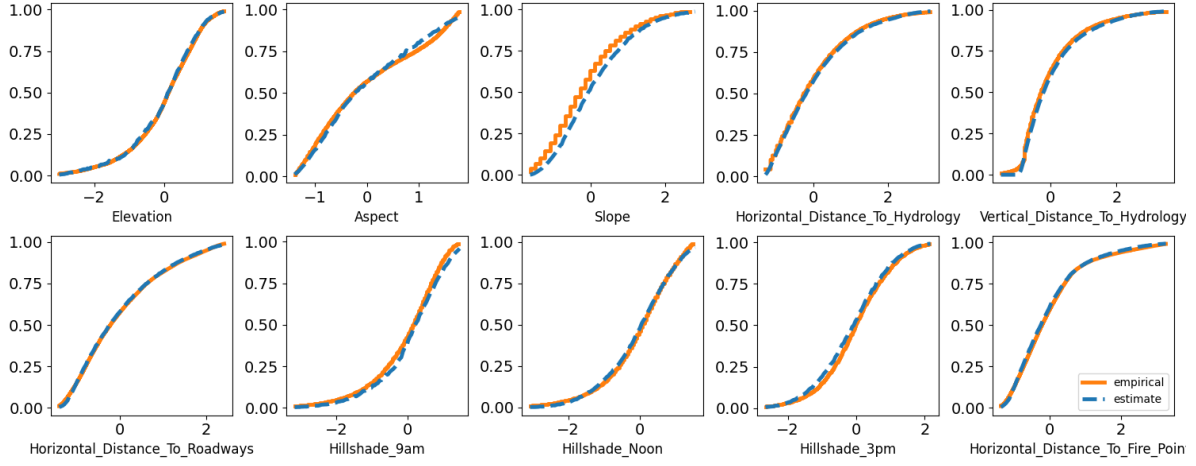
Table 9: The number of model parameters for tabular dataset experiments.

Model	covtype	credit	adult	loan	cabs	kings
CTGAN	20k	32k	52k	13k	30k	51k
TVAE	10k	12k	13k	6k	10k	10k
CTAB-GAN	12k	13k	14k	5k	12k	15k
DistVAE	10k	12k	13k	6k	10k	16k

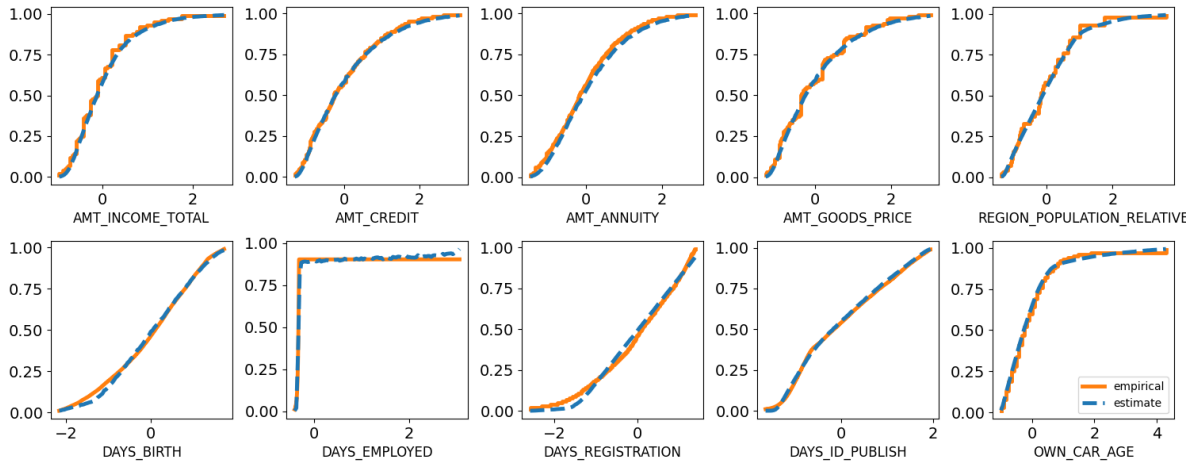
Table 10: Classifier and regressor used in the evaluation of synthetic data quality. The names of all parameters used in the description are consistent with those defined in corresponding packages.

Tasks	Model	Description
Regression	Linear Regression	Package: <code>statsmodels.api.sm.OLS</code> , setting: without intercept, defaulted values
	Random Forest	Package: <code>sklearn.ensemble.RandomForestRegressor</code> , setting: <code>random_state=0</code> , defaulted values
	Gradient Boosting	Package: <code>sklearn.ensemble.GradientBoostingRegressor</code> , setting: <code>random_state=0</code> , defaulted values
Classification	Logistic Regression	Package: <code>sklearn.linear_model.LogisticRegression</code> , setting: <code>multi_class='ovr'</code> , <code>fit_intercept=False</code> , defaulted values
	Random Forest	Package: <code>sklearn.ensemble.RandomForestClassifier</code> , setting: <code>random_state=0</code> , defaulted values
	Gradient Boosting	Package: <code>sklearn.ensemble.GradientBoostingClassifier</code> , setting: <code>random_state=0</code> , defaulted values

## A.9 Detailed Experimental Results



(a) `covtype`



(b) `credit`

Figure 3: Estimated CDFs of continuous covariates ( $B = 5000$ ). We standardize continuous variables to compare the estimated CDF within a comparable range.

Table 11: Machine learning utilities for synthetic datasets. Mean and standard deviation values are obtained from 10 repeated experiments.  $\uparrow$  denotes higher is better and  $\downarrow$  denotes lower is better.

(a)						
Dataset	coverttype		credit		loan	
Model	MARE $\downarrow$	$F_1$ $\uparrow$	MARE $\downarrow$	$F_1$ $\uparrow$	MARE $\downarrow$	$F_1$ $\uparrow$
Baseline	0.035	0.718	0.064	0.927	0.020	0.948
CTGAN	$0.058_{\pm 0.007}$	$0.227_{\pm 0.030}$	$0.593_{\pm 0.150}$	$0.914_{\pm 0.006}$	$0.258_{\pm 0.020}$	$0.842_{\pm 0.109}$
TVAE	$0.079_{\pm 0.007}$	$0.504_{\pm 0.032}$	$0.260_{\pm 0.135}$	$0.091_{\pm 0.286}$	$0.124_{\pm 0.033}$	$0.785_{\pm 0.288}$
CTAB-GAN	$0.065_{\pm 0.004}$	$0.493_{\pm 0.027}$	$0.887_{\pm 0.351}$	$0.913_{\pm 0.005}$	$0.247_{\pm 0.019}$	$0.887_{\pm 0.026}$
DistVAE( $\beta = 0.5$ )	$0.044_{\pm 0.002}$	$0.605_{\pm 0.006}$	$0.763_{\pm 0.068}$	$0.926_{\pm 0.001}$	$0.249_{\pm 0.007}$	$0.914_{\pm 0.009}$

(b)						
Dataset	adult		cabs		kings	
Model	MARE $\downarrow$	$F_1$ $\uparrow$	MARE $\downarrow$	$F_1$ $\uparrow$	MARE $\downarrow$	$F_1$ $\uparrow$
Baseline	0.216	0.854	0.565	0.743	0.001	0.695
CTGAN	$0.297_{\pm 0.030}$	$0.796_{\pm 0.022}$	$0.721_{\pm 0.046}$	$0.674_{\pm 0.024}$	$0.001_{\pm 0.000}$	$0.579_{\pm 0.035}$
TVAE	$0.238_{\pm 0.006}$	$0.809_{\pm 0.016}$	$0.642_{\pm 0.035}$	$0.689_{\pm 0.031}$	$0.010_{\pm 0.005}$	$0.687_{\pm 0.041}$
CTAB-GAN	$0.321_{\pm 0.036}$	$0.730_{\pm 0.069}$	$0.894_{\pm 0.116}$	$0.582_{\pm 0.047}$	$0.001_{\pm 0.000}$	$0.608_{\pm 0.022}$
DistVAE( $\beta = 0.5$ )	$0.232_{\pm 0.004}$	$0.825_{\pm 0.009}$	$0.803_{\pm 0.129}$	$0.707_{\pm 0.010}$	$0.001_{\pm 0.000}$	$0.640_{\pm 0.002}$

Table 12: Statistical similarity of synthetic datasets. K-S represents the Kolmogorov–Smirnov statistic and 1-WD represents the 1-Wasserstein distance. Mean and standard deviation values are obtained from 10 repeated experiments.  $\downarrow$  means lower is better.

(a) Continuous						
Dataset	covertype		credit		loan	
Model	K-S $\downarrow$	1-WD $\downarrow$	K-S $\downarrow$	1-WD $\downarrow$	K-S $\downarrow$	1-WD $\downarrow$
CTGAN	0.080 $\pm$ 0.011	0.108 $\pm$ 0.014	0.132 $\pm$ 0.017	0.088 $\pm$ 0.013	0.112 $\pm$ 0.055	0.061 $\pm$ 0.016
TVAE	0.088 $\pm$ 0.008	0.156 $\pm$ 0.018	0.156 $\pm$ 0.036	0.200 $\pm$ 0.035	0.162 $\pm$ 0.024	0.201 $\pm$ 0.024
CTAB-GAN	0.073 $\pm$ 0.011	0.096 $\pm$ 0.014	0.140 $\pm$ 0.021	0.111 $\pm$ 0.013	0.181 $\pm$ 0.070	0.153 $\pm$ 0.023
DistVAE( $\beta = 0.5$ )	0.032 $\pm$ 0.003	0.041 $\pm$ 0.005	0.088 $\pm$ 0.014	0.089 $\pm$ 0.004	0.060 $\pm$ 0.010	0.048 $\pm$ 0.003
(b) Continuous						
Dataset	adult		cabs		kings	
Model	K-S $\downarrow$	1-WD $\downarrow$	K-S $\downarrow$	1-WD $\downarrow$	K-S $\downarrow$	1-WD $\downarrow$
CTGAN	0.323 $\pm$ 0.126	0.086 $\pm$ 0.017	0.045 $\pm$ 0.007	0.060 $\pm$ 0.011	0.109 $\pm$ 0.012	0.116 $\pm$ 0.016
TVAE	0.477 $\pm$ 0.053	0.414 $\pm$ 0.070	0.098 $\pm$ 0.008	0.139 $\pm$ 0.023	0.195 $\pm$ 0.018	0.213 $\pm$ 0.046
CTAB-GAN	0.275 $\pm$ 0.122	0.178 $\pm$ 0.053	0.086 $\pm$ 0.008	0.118 $\pm$ 0.015	0.188 $\pm$ 0.035	0.128 $\pm$ 0.019
DistVAE( $\beta = 0.5$ )	0.209 $\pm$ 0.064	0.114 $\pm$ 0.009	0.044 $\pm$ 0.003	0.067 $\pm$ 0.003	0.110 $\pm$ 0.008	0.089 $\pm$ 0.003
(c) Discrete						
Dataset	covertype		credit		loan	
Model	K-S $\downarrow$	1-WD $\downarrow$	K-S $\downarrow$	1-WD $\downarrow$	K-S $\downarrow$	1-WD $\downarrow$
CTGAN	0.591 $\pm$ 0.003	1.629 $\pm$ 0.011	0.061 $\pm$ 0.008	0.147 $\pm$ 0.024	0.070 $\pm$ 0.010	0.076 $\pm$ 0.013
TVAE	0.238 $\pm$ 0.042	0.606 $\pm$ 0.033	0.583 $\pm$ 0.045	1.566 $\pm$ 0.116	0.193 $\pm$ 0.028	0.221 $\pm$ 0.043
CTAB-GAN	0.052 $\pm$ 0.028	0.180 $\pm$ 0.126	0.034 $\pm$ 0.006	0.076 $\pm$ 0.018	0.039 $\pm$ 0.011	0.046 $\pm$ 0.013
DistVAE( $\beta = 0.5$ )	0.023 $\pm$ 0.010	0.073 $\pm$ 0.046	0.020 $\pm$ 0.003	0.046 $\pm$ 0.006	0.019 $\pm$ 0.005	0.027 $\pm$ 0.008
(d) Discrete						
Dataset	adult		cabs		kings	
Model	K-S $\downarrow$	1-WD $\downarrow$	K-S $\downarrow$	1-WD $\downarrow$	K-S $\downarrow$	1-WD $\downarrow$
CTGAN	0.065 $\pm$ 0.008	0.463 $\pm$ 0.051	0.069 $\pm$ 0.016	0.238 $\pm$ 0.036	0.140 $\pm$ 0.018	0.529 $\pm$ 0.064
TVAE	0.479 $\pm$ 0.048	5.228 $\pm$ 0.273	0.411 $\pm$ 0.088	1.202 $\pm$ 0.212	0.405 $\pm$ 0.034	1.262 $\pm$ 0.099
CTAB-GAN	0.169 $\pm$ 0.018	0.745 $\pm$ 0.294	0.086 $\pm$ 0.013	0.443 $\pm$ 0.074	0.255 $\pm$ 0.027	0.979 $\pm$ 0.107
DistVAE( $\beta = 0.5$ )	0.037 $\pm$ 0.004	0.248 $\pm$ 0.026	0.060 $\pm$ 0.017	0.241 $\pm$ 0.084	0.022 $\pm$ 0.004	0.071 $\pm$ 0.012

Table 13: Privacy preservability: Distance to closest record for all tabular datasets between real and synthetic data (R&S) and within real data (R) and synthetic data (S). Mean and standard deviation values are obtained from 10 repeated experiments. Higher is better.

(a)				(b)			
Dataset		covertime		Dataset		credit	
Model	R&S	R	S	Model	R&S	R	S
CTGAN	0.715 $\pm$ 0.026	0.329 $\pm$ 0.000	0.514 $\pm$ 0.094	CTGAN	0.624 $\pm$ 0.033	0.452 $\pm$ 0.000	0.592 $\pm$ 0.061
TVAE	0.676 $\pm$ 0.031	0.329 $\pm$ 0.000	0.482 $\pm$ 0.025	TVAE	0.627 $\pm$ 0.118	0.452 $\pm$ 0.000	0.423 $\pm$ 0.212
CTAB-GAN	0.892 $\pm$ 0.031	0.329 $\pm$ 0.000	0.011 $\pm$ 0.005	CTAB-GAN	0.715 $\pm$ 0.025	0.452 $\pm$ 0.000	0.014 $\pm$ 0.006
DistVAE( $\beta = 0.5$ )	0.765 $\pm$ 0.008	0.329 $\pm$ 0.000	0.819 $\pm$ 0.010	DistVAE( $\beta = 0.5$ )	0.692 $\pm$ 0.012	0.452 $\pm$ 0.000	0.742 $\pm$ 0.012
DistVAE( $\beta = 1$ )	0.878 $\pm$ 0.008	0.329 $\pm$ 0.000	0.906 $\pm$ 0.009	DistVAE( $\beta = 1$ )	0.700 $\pm$ 0.006	0.452 $\pm$ 0.000	0.750 $\pm$ 0.005
DistVAE( $\beta = 5$ )	0.907 $\pm$ 0.012	0.329 $\pm$ 0.000	0.939 $\pm$ 0.008	DistVAE( $\beta = 5$ )	0.718 $\pm$ 0.007	0.452 $\pm$ 0.000	0.757 $\pm$ 0.007

(c)				(d)			
Dataset		loan		Dataset		adult	
Model	R&S	R	S	Model	R&S	R	S
CTGAN	0.249 $\pm$ 0.017	0.109 $\pm$ 0.000	0.243 $\pm$ 0.024	CTGAN	0.063 $\pm$ 0.017	0.000 $\pm$ 0.000	0.000 $\pm$ 0.000
TVAE	0.298 $\pm$ 0.057	0.109 $\pm$ 0.000	0.154 $\pm$ 0.026	TVAE	0.277 $\pm$ 0.039	0.000 $\pm$ 0.000	0.000 $\pm$ 0.000
CTAB-GAN	0.272 $\pm$ 0.024	0.109 $\pm$ 0.000	0.076 $\pm$ 0.051	CTAB-GAN	0.152 $\pm$ 0.064	0.000 $\pm$ 0.000	0.000 $\pm$ 0.000
DistVAE( $\beta = 0.5$ )	0.244 $\pm$ 0.025	0.109 $\pm$ 0.000	0.245 $\pm$ 0.020	DistVAE( $\beta = 0.5$ )	0.060 $\pm$ 0.040	0.000 $\pm$ 0.000	0.005 $\pm$ 0.001
DistVAE( $\beta = 1$ )	0.238 $\pm$ 0.019	0.109 $\pm$ 0.000	0.241 $\pm$ 0.023	DistVAE( $\beta = 1$ )	0.048 $\pm$ 0.027	0.000 $\pm$ 0.000	0.003 $\pm$ 0.000
DistVAE( $\beta = 5$ )	0.243 $\pm$ 0.015	0.109 $\pm$ 0.000	0.240 $\pm$ 0.025	DistVAE( $\beta = 5$ )	0.177 $\pm$ 0.002	0.000 $\pm$ 0.000	0.001 $\pm$ 0.000

(e)				(f)			
Dataset		cabs		Dataset		kings	
Model	R&S	R	S	Model	R&S	R	S
CTGAN	0.353 $\pm$ 0.006	0.332 $\pm$ 0.000	0.341 $\pm$ 0.010	CTGAN	0.550 $\pm$ 0.016	0.199 $\pm$ 0.000	0.447 $\pm$ 0.030
TVAE	0.339 $\pm$ 0.008	0.332 $\pm$ 0.000	0.195 $\pm$ 0.015	TVAE	0.603 $\pm$ 0.091	0.199 $\pm$ 0.000	0.414 $\pm$ 0.053
CTAB-GAN	0.423 $\pm$ 0.025	0.332 $\pm$ 0.000	0.012 $\pm$ 0.023	CTAB-GAN	0.596 $\pm$ 0.030	0.199 $\pm$ 0.000	0.122 $\pm$ 0.135
DistVAE( $\beta = 0.5$ )	0.364 $\pm$ 0.004	0.332 $\pm$ 0.000	0.368 $\pm$ 0.005	DistVAE( $\beta = 0.5$ )	0.540 $\pm$ 0.009	0.199 $\pm$ 0.000	0.600 $\pm$ 0.013
DistVAE( $\beta = 1$ )	0.364 $\pm$ 0.004	0.332 $\pm$ 0.000	0.367 $\pm$ 0.004	DistVAE( $\beta = 1$ )	0.552 $\pm$ 0.008	0.199 $\pm$ 0.000	0.605 $\pm$ 0.014
DistVAE( $\beta = 5$ )	0.368 $\pm$ 0.003	0.332 $\pm$ 0.000	0.365 $\pm$ 0.005	DistVAE( $\beta = 5$ )	0.692 $\pm$ 0.013	0.199 $\pm$ 0.000	0.763 $\pm$ 0.015

Table 14: Privacy preservability: Membership inference attack performance for all tabular datasets. Mean and standard deviation values are obtained from 10 repeated experiments. Lower is better.

(a)			(b)		
Dataset	covertime		Dataset	credit	
Model	Accuracy	AUC	Model	Accuracy	AUC
TVAE	$0.499_{\pm 0.007}$	$0.499_{\pm 0.007}$	TVAE	$0.500_{\pm 0.001}$	$0.500_{\pm 0.001}$
DistVAE( $\beta = 0.5$ )	$0.500_{\pm 0.003}$	$0.500_{\pm 0.003}$	DistVAE( $\beta = 0.5$ )	$0.500_{\pm 0.001}$	$0.500_{\pm 0.001}$
(c)			(d)		
Dataset	loan		Dataset	adult	
Model	Accuracy	AUC	Model	Accuracy	AUC
TVAE	$0.497_{\pm 0.015}$	$0.497_{\pm 0.015}$	TVAE	$0.493_{\pm 0.017}$	$0.493_{\pm 0.017}$
DistVAE( $\beta = 0.5$ )	$0.502_{\pm 0.006}$	$0.502_{\pm 0.006}$	DistVAE( $\beta = 0.5$ )	$0.500_{\pm 0.000}$	$0.500_{\pm 0.000}$
(e)			(f)		
Dataset	cabs		Dataset	kings	
Model	Accuracy	AUC	Model	Accuracy	AUC
TVAE	$0.480_{\pm 0.033}$	$0.480_{\pm 0.033}$	TVAE	$0.507_{\pm 0.025}$	$0.507_{\pm 0.025}$
DistVAE( $\beta = 0.5$ )	$0.498_{\pm 0.003}$	$0.498_{\pm 0.003}$	DistVAE( $\beta = 0.5$ )	$0.502_{\pm 0.004}$	$0.502_{\pm 0.004}$

Table 15: Privacy preservability: Attribute disclosure performance for all tabular datasets. Mean and standard deviation values are obtained from 10 repeated experiments. Lower is better.

(a) <b>covtype</b>				(b) <b>credit</b>			
Model	Number of neighbors ( $k$ )			Model	Number of neighbors ( $k$ )		
	1	10	100		1	10	100
CTGAN	0.161 $\pm$ 0.030	0.175 $\pm$ 0.029	0.155 $\pm$ 0.041	CTGAN	0.319 $\pm$ 0.009	0.330 $\pm$ 0.009	0.323 $\pm$ 0.011
TVAE	0.356 $\pm$ 0.086	0.357 $\pm$ 0.091	0.349 $\pm$ 0.094	TVAE	0.615 $\pm$ 0.147	0.618 $\pm$ 0.143	0.614 $\pm$ 0.145
CTAB-GAN	0.200 $\pm$ 0.035	0.225 $\pm$ 0.042	0.238 $\pm$ 0.033	CTAB-GAN	0.322 $\pm$ 0.007	0.332 $\pm$ 0.012	0.331 $\pm$ 0.010
DistVAE( $\beta = 0.5$ )	0.308 $\pm$ 0.025	0.338 $\pm$ 0.037	0.313 $\pm$ 0.035	DistVAE( $\beta = 0.5$ )	0.339 $\pm$ 0.013	0.337 $\pm$ 0.011	0.315 $\pm$ 0.012
DistVAE( $\beta = 1$ )	0.264 $\pm$ 0.024	0.294 $\pm$ 0.036	0.282 $\pm$ 0.029	DistVAE( $\beta = 1$ )	0.339 $\pm$ 0.010	0.324 $\pm$ 0.005	0.301 $\pm$ 0.004
DistVAE( $\beta = 5$ )	0.141 $\pm$ 0.019	0.135 $\pm$ 0.013	0.115 $\pm$ 0.011	DistVAE( $\beta = 5$ )	0.332 $\pm$ 0.007	0.317 $\pm$ 0.007	0.293 $\pm$ 0.007

(c) <b>loan</b>				(d) <b>adult</b>			
Model	Number of neighbors ( $k$ )			Model	Number of neighbors ( $k$ )		
	1	10	100		1	10	100
CTGAN	0.439 $\pm$ 0.027	0.447 $\pm$ 0.022	0.426 $\pm$ 0.033	CTGAN	0.234 $\pm$ 0.012	0.255 $\pm$ 0.021	0.261 $\pm$ 0.023
TVAE	0.611 $\pm$ 0.153	0.602 $\pm$ 0.152	0.596 $\pm$ 0.157	TVAE	0.318 $\pm$ 0.081	0.318 $\pm$ 0.080	0.307 $\pm$ 0.080
CTAB-GAN	0.475 $\pm$ 0.048	0.443 $\pm$ 0.027	0.435 $\pm$ 0.030	CTAB-GAN	0.199 $\pm$ 0.032	0.202 $\pm$ 0.032	0.205 $\pm$ 0.031
DistVAE( $\beta = 0.5$ )	0.505 $\pm$ 0.043	0.465 $\pm$ 0.038	0.439 $\pm$ 0.032	DistVAE( $\beta = 0.5$ )	0.270 $\pm$ 0.018	0.280 $\pm$ 0.021	0.268 $\pm$ 0.015
DistVAE( $\beta = 1$ )	0.449 $\pm$ 0.038	0.440 $\pm$ 0.035	0.423 $\pm$ 0.031	DistVAE( $\beta = 1$ )	0.264 $\pm$ 0.006	0.276 $\pm$ 0.005	0.260 $\pm$ 0.007
DistVAE( $\beta = 5$ )	0.458 $\pm$ 0.013	0.441 $\pm$ 0.035	0.416 $\pm$ 0.031	DistVAE( $\beta = 5$ )	0.205 $\pm$ 0.005	0.187 $\pm$ 0.003	0.166 $\pm$ 0.002

(e) <b>cabs</b>				(f) <b>kings</b>			
Model	Number of neighbors ( $k$ )			Model	Number of neighbors ( $k$ )		
	1	10	100		1	10	100
CTGAN	0.238 $\pm$ 0.009	0.246 $\pm$ 0.006	0.231 $\pm$ 0.010	CTGAN	0.200 $\pm$ 0.009	0.257 $\pm$ 0.032	0.269 $\pm$ 0.036
TVAE	0.385 $\pm$ 0.079	0.383 $\pm$ 0.079	0.381 $\pm$ 0.081	TVAE	0.338 $\pm$ 0.045	0.349 $\pm$ 0.046	0.345 $\pm$ 0.044
CTAB-GAN	0.235 $\pm$ 0.010	0.236 $\pm$ 0.008	0.237 $\pm$ 0.011	CTAB-GAN	0.111 $\pm$ 0.068	0.111 $\pm$ 0.088	0.123 $\pm$ 0.114
DistVAE( $\beta = 0.5$ )	0.251 $\pm$ 0.010	0.241 $\pm$ 0.007	0.225 $\pm$ 0.005	DistVAE( $\beta = 0.5$ )	0.293 $\pm$ 0.019	0.310 $\pm$ 0.041	0.301 $\pm$ 0.050
DistVAE( $\beta = 1$ )	0.246 $\pm$ 0.010	0.240 $\pm$ 0.006	0.227 $\pm$ 0.008	DistVAE( $\beta = 1$ )	0.281 $\pm$ 0.016	0.306 $\pm$ 0.039	0.290 $\pm$ 0.041
DistVAE( $\beta = 5$ )	0.238 $\pm$ 0.010	0.220 $\pm$ 0.009	0.199 $\pm$ 0.005	DistVAE( $\beta = 5$ )	0.215 $\pm$ 0.010	0.221 $\pm$ 0.036	0.205 $\pm$ 0.038